Project	AtlantOS – 633211
Deliverable number	D7.16
Deliverable title	Assessment of AtlantOS impact
Description	Assessment of the impact of AtlantOS in situ observing system for Copernicus Marine Service and seasonal prediction
Work Package number	WP7
Work Package title	Integration in models and impact
Lead beneficiary	Mercator Ocean
Lead authors	Elisabeth Rémy (Mercator Ocean)
Contributors	Robert King (Met Office), Chongyuan Mao (Met Office), Stéphanie Guinehut (CLS), Hao Zuo (ECMWF), Michael Mayer (ECMWF), Beena Balan Sarojini (ECMWF), Florent Gasparin (Mercator Océan), Mathieu Hamon (Mercator Océan)
Submission data	17 December 2018, 18 March 2020 (updated)
Due date	1st September 2018
Comments	

This project has received funding from the European Union's Horizon 2020 research and innovation program under grant agreement n° 633211.

Stakeholder engagement relating to this task*

WHO are your most important stakeholders?	x Private company If yes, is it an SME x or a large company ☐? x National governmental body x International organization ☐ NGO ☐ others Please give the name(s) of the stakeholder(s): ECMWF, Met Office, CLS, Mercator Ocean, Copernicus Marine and Climate Service, Coriolis, EuroArgo
WHERE is/are the company(ies) or organization(s) from?	x Your own country x Another country in the EU ☐ Another country outside the EU Please name the country(ies): France, UK
Is this deliverable a success story? If yes, why? **If not, why?**	x Yes, the impact of the deep Argo and surface drifter observations integration into different Copernicus Marine ocean monitoring and Copernicus Climate seasonal prediction systems was assessed, giving a broad view of their benefit in improving ocean and atmosphere estimates. ☐ No, because …..
Will this deliverable be used? **If yes, who will use it?** **If not, why will it not be used?**	x Yes, this deliverable will be made available and results presented within the Copernicus Marine, Climate Service and GODAE OceanView communities as well as discussed with the in situ observation network providers. ☐ No, because …..

NOTE: This information is being collected for the following purposes:

1. To make a list of all companies/organizations with which AtlantOS partners have had contact. This is important to demonstrate the extent of industry and public-sector collaboration in the obs community. Please note that we will only publish one aggregated list of companies and not mention specific partnerships.
2. To better report success stories from the AtlantOS community on how observing delivers concrete value to society.

*For ideas about relations with stakeholders you are invited to consult D10.5 Best Practices in Stakeholder Engagement, Data Dissemination and Exploitation.

Contenu

WP7 – T7.4 Integration in models and impact

This report gathers the contributions of the different partners (CLS, MetOffice, Mercator Ocean and ECMWF) within the Task 7.4 on the assessment of the impact of near real time AtlantOS observations for the Copernicus Marine Service ocean analysis and forecasts and seasonal forecasts. This Task 7.4 complement the Task 1.3 that assessed the improvements for the Copernicus Marine Service expected from the future evolution of AtlantOS networks.

Impact for data assimilation is using Observing System Evaluations and other alternative techniques (e.g. influence matrices). These impact studies are taking into account synergy with satellite observations as they rely on data assimilation systems that merge in-situ observations together with satellite observations.

Based on the inputs from the in situ networks involved in WP2 and WP3, impact studies have been defined depending on the status of the platform deployments, their availability and quality.

1 Introduction

Operational systems from MetOffice, Mercator-Ocean, CLS and ECMWF have been used to make assessments of the value of various in-situ observations. All of those systems are assimilating at least sea level observations, satellite SST and in situ temperature and salinity profiles. In the context of seasonal forecast, here is considered the impact of Ocean Initial Conditions that were obtained without some part of the ocean in situ observations on atmospheric estimate from seasonal forecasts.

For the ocean, the different group mainly focus on the impact of the deep Argo profilers and surface drifters.

The Argo network currently comprises around 4000 autonomous floats which profile the temperature and salinity of the world's ocean down to 2000m depth, providing reasonably uniform coverage in space and time. This marked increase in sub-surface observation sampling over the past two decades has proven invaluable for short-term forecasting and long-term monitoring of the ocean (Balmaseda et al. 2007; Oke & Schiller 2007, Turpin et al. 2016). More recently, new float technologies have allowed the Argo network to extend to depths of up to 4000m and 6000m (Jayne et al. 2017). Through AtlantOS a number of deep Argo floats have been deployed and their measurements relayed for use in operational systems. A small number of deep Argo floats are relaying observations in NRT and have been assimilated into the Met Office operational global forecasting system. This is not the case for the Mercator Ocean and ARMOR3D systems that did not assimilate the deep part of the profiles due to QC flags set to 2 and 3. Specific experiments were then conducted assimilating those deep profiles.

Unlike the deep ocean, there is a relative wealth of surface temperature observations which are routinely assimilated into the Met Office, Mercator Ocean and ARMOR3D operational ocean monitoring systems. This includes satellite observations of the sea surface temperature (SST) and in situ measurements from ships, fixed platforms and buoys. Surface drifters are only assimilated in the MetOffice ocean forecasting system. As part of AtlantOS there has been work to deploy additional surface drifters. While the impact of small number additional SST observations would be expected to be minimal, accurate in situ SST measurements play a crucial role in the bias correction of satellite measurements.
At MetOffice, this affects both the ocean forecasting systems and the operational SST analysis (OSTIA) which is widely used by other ocean forecasting centres, including Mercator Ocean, and as the boundary condition for the Met Office and ECMWF numerical weather prediction (NWP) systems.

To assess the impact of surface drifters on ocean analysis and forecasts, dedicated experiments where conducted with the MetOffice and Mercator Ocean systems.

In each section is given a brief description of the system considered, the assimilation experiment setup and then the impact assessment analysis.

2 Impact of AtlantOS network in the MetOffice global ocean analysis and forecasting system

A model-observation comparison was conducted to assess the observations in the almost-unconstrained deep ocean to determine the extent to which the model retains this information.

Short-term observing system experiments were performed to determine the impact of the existing network of surface drifters. To do this, three experiments using the full drifter network, and 2 others with-holding 20% and 50% of drifters are compared.

2.1 Ocean forecasting system description

The UK Met Office runs an operational global ocean analysis and forecasting system, providing daily analyses and 7-day forecasts of the 3-D ocean temperature, salinity, currents, and sea surface height. This system runs every day and uses a 75-vertical level, 0.25 degree global ocean configuration forced by 3-hourly Met Office NWP fluxes. Using a 24-hour assimilation window, we assimilate observations of the sea surface temperature (SST), sea level anomaly (SLA), sea-ice concentration (SIC), and in situ measurements of temperature and salinity.

We assimilate swath SST observations from several satellites available through GHRSST in addition to SST measurements from in situ platforms, ships, and drifting buoys distributed over the global telecommunications service (GTS). The assimilated in situ sub-surface measurements of temperature and salinity (available over the GTS) include observations from the Argo array, XBTs, CTDs, gliders, moored buoys and marine mammals. We also assimilate along-track SLA observations provided through CMEMS and sea-ice concentration measurements provided by OSI-SAF.

This system is being used in AtlantOS WP1-task1.3 to perform observing system simulation experiments (OSSEs) designed to investigate the potential impact of extensions to the existing Atlantic observing network. Similarly here, the Met Office operational system will be used to investigate the use of new AtlantOS observations made available for use in real-time systems.

2.2 Impact of Deep Argo Observations

Method

Measurements below 2000 m from Deep Argo floats have been assimilated into the operational global ocean analysis since February 2018. A total of 8 Deep Argo floats have been assimilated in the Atlantic during March – August 2018, within which six floats were deployed in 2018. This report aims to assess the impact of Deep Argo on FOAM by comparing the initial and latest appearance in the model. Two of the Atlantic floats were deployed in 2017 but were not properly assimilated before March 2018 as a result of

model upgrade and observation data format update. We thus focus on the six Atlantic floats deployed in 2018 (Figure 1) and the information of these Atlantic floats are listed in Table 1.

Table 1. Information of the Deep Argo floats deployed in 2018 in the Atlantic domain

Argo ID	Location[1]	First date in Model	Last Date in Model	Report Frequency
6901601	59.8 °N, 35.0 °W	25 July 2018	24 August 2018	10 days
3902126	29.1 °N, 17.7 °W	20 April 2018	30 August 2018	3 days
3902128	23.98°S, 8.3 °W	24 March 2018	24 August 2018	3 days
3902130	24.3 °S, 2.1 °W	2 April 2018	24 August 2018	3 days
3902131	6.6 °S, 5.6 °E	15 March 2018	22 August 2018	3 days
3902132	0.1 °, 9.4 °W	10 April 2018	22 August 2018	3 days

[1] The location is the mean latitude and longitude of the Argo float during March – August 2018

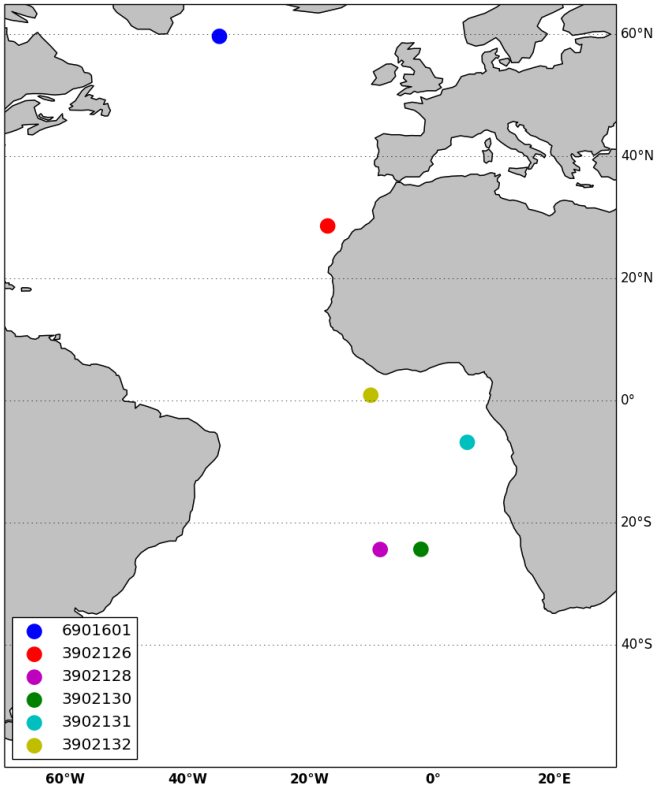

Figure 1: Location of six Deep Argo floats deployed in the Atlantic in 2018

2.2.1 Impact

The Deep Argo floats are not expected to drift significantly and so provide repeated measurements of the water column. Each time the observations are assimilated into an ocean model, the estimate of deep ocean state is expected to improve. Figure 2 shows the trajectory (Figure 2a and 2c) and profiles (Figure 2b and 2d) of the temperature and salinity observations from Float 3902126. In Figure 2b and 2d, the left panels are the first time observations were assimilated into the model and hence show a larger discrepancy between observation and model. By assimilating the observations over the following months at locations

within 1° radius, the differences between observations and model background are much smaller (see middle panels in Figure 2b and 2d). The observation minus background (O-B) shown in the right panels highlight the change with the O-B for the last assimilation (solid red line) much closer to zero line than the first assimilation (dashed red line), especially below 2000 m. The colours for the trajectories are the averaged O-B for temperature (Figure 2a) and salinity (Figure 2c) over depths below 2000 m. For temperature, there are slight stronger variations in O-B but the later profiles pull the model background closer to observations. On the other hand, the salinity O-B is close to zero through most cycles, except for three profiles where both temperature and salinity show negative O-B values potentially due to bad observations.

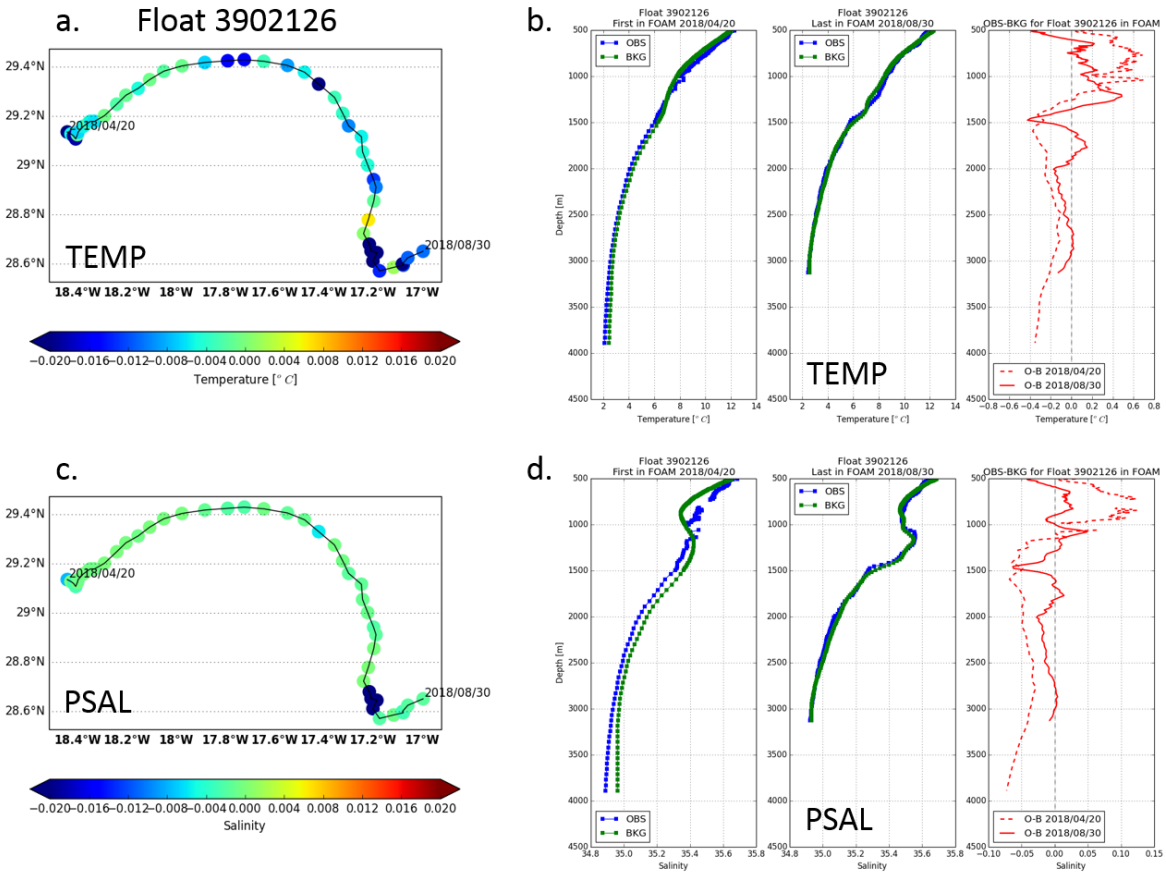

Figure 2. Trajectory and profiles for Float 3902126: a. temperature profile trajectory with colour indicating the average observation-minus-background (O-B) for depths below 3000 m, b. temperature observation (blue) and model background (green) profiles for the first assimilation (left), last assimilation (middle) and O-B of the two assimilations (dashed red line is first assimilation and solid red line is last assimilation), c. the same as a but for salinity and d. the same as b but for salinity.

Similar trajectory and profiles are shown in Figure 3 and Figure 4 for Float 3902128 and Float 6901601. For Float 3902128, the average O-B values for both temperature (Figure 3a) and salinity (Figure 3c) are close to zero from the first assimilation. The profiles demonstrate that by assimilating observations from Deep Argo, the O-B values over the water column also move closer to zero. For example, the temperature profile (Figure 3b, right panel) shows a discrepancy between observation and model background at ~600 m of -0.45 °C when the profile was first assimilated in March. This discrepancy has been largely reduced to ~0.1 °C when it was assimilated last time in August.

Float 6901601 reports measurements less frequently than the two floats shown above, during the first month of deployment since July there were 4 profiles assimilated into the model. These 4 profiles still help the pull the model closer to the observations and reduce the O-B values (Figure 4b and 4d, right panels).

The reporting depths varies during the cycles (see http://www.usgodae.org/cgi-bin/argo_select.pl for example profiles), but its impact over the depths with valid observations is satisfying.

The trajectory and profiles of floats 3902130, 3902131 and 3902132 are shown in Figure 5-7. The results are similar to the three floats described above so are not repeated in detail here.

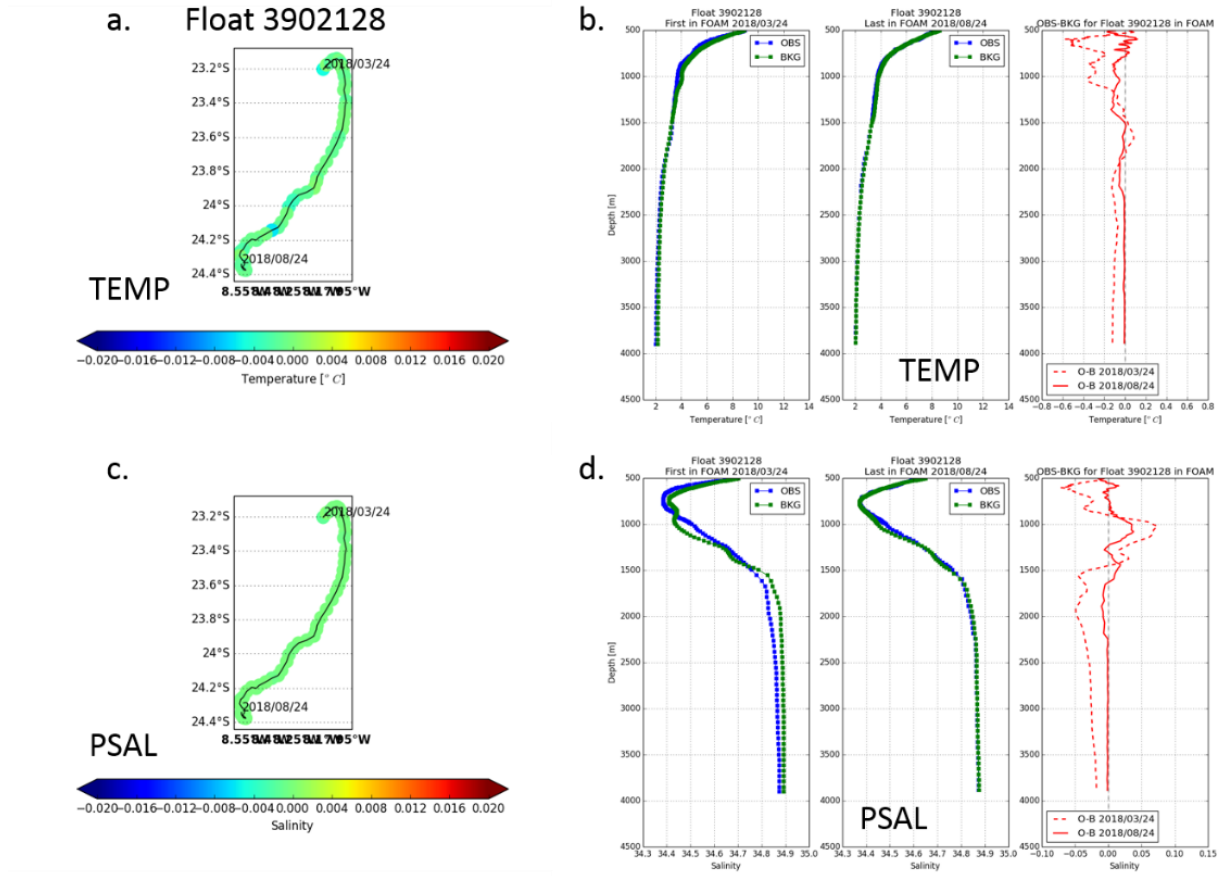

Figure 3. Trajectory and profiles for Float 3902128: a. temperature profile trajectory with colour indicating the average observation-minus-background (O-B) for depths below 3000 m, b. temperature observation (blue) and model background (green) profiles for the first assimilation (left), last assimilation (middle) and O-B of the two assimilations (dashed red line is first assimilation and solid red line is last assimilation), c. the same as a but for salinity and d. the same as b but for salinity.

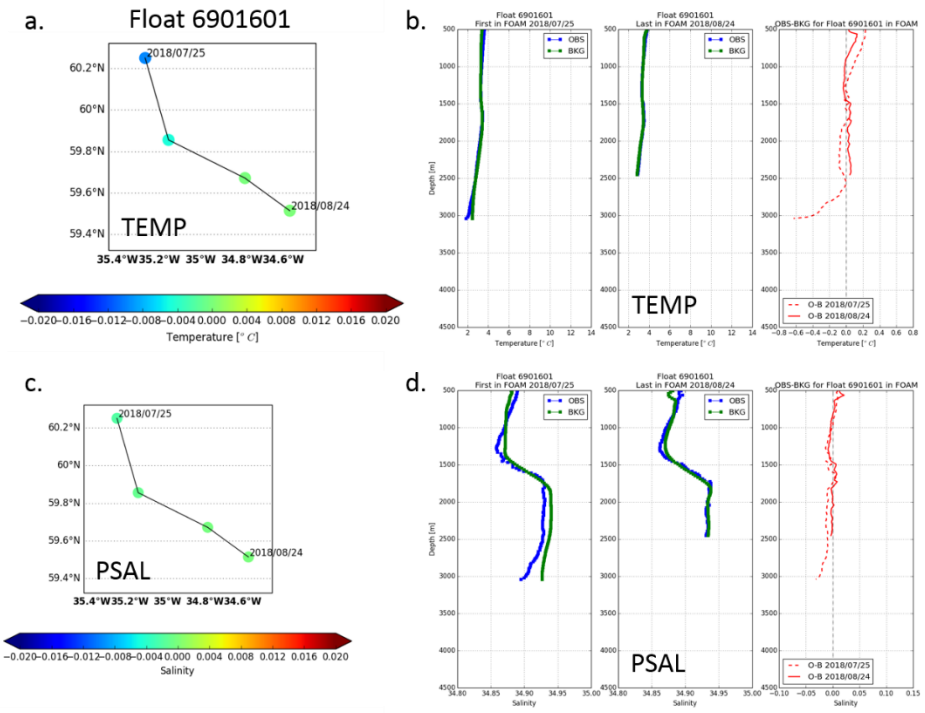

Figure 4. Trajectory and profiles for Float 6901601: a. temperature profile trajectory with colour indicating the average observation-minus-background (O-B) for depths below 3000 m, b. temperature observation (blue) and model background (green) profiles for the first assimilation (left), last assimilation (middle) and O-B of the two assimilations (dashed red line is first assimilation and solid red line is last assimilation), c. the same as a but for salinity and d. the same as b but for salinity.

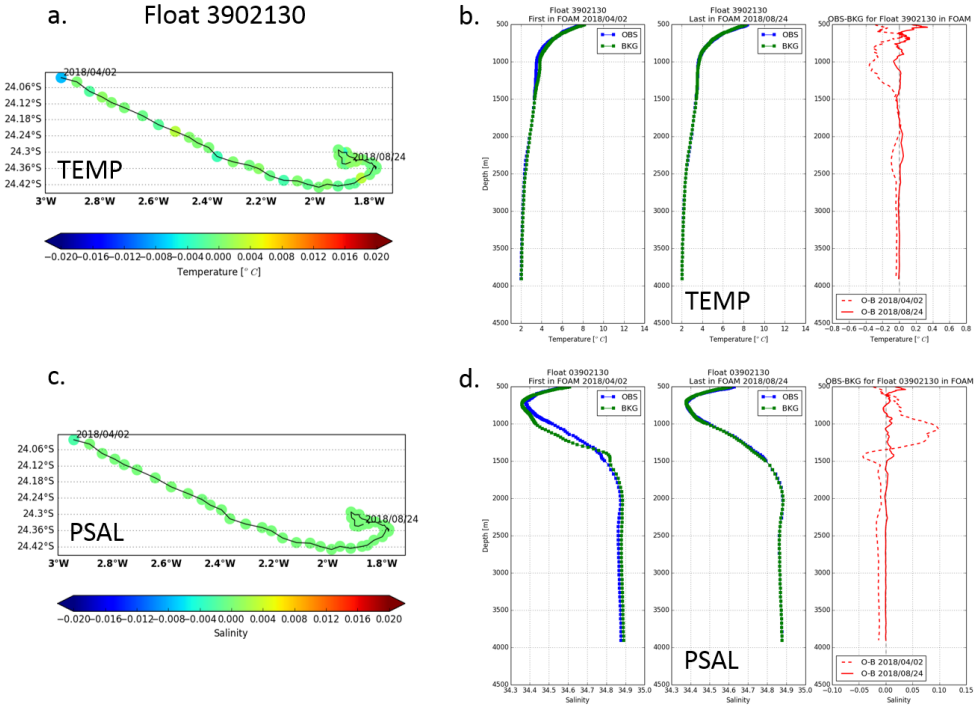

Figure 5. Trajectory and profiles for Float 3902130: a. temperature profile trajectory with colour indicating the average observation-minus-background (O-B) for depths below 3000 m, b. temperature observation (blue) and model background (green) profiles for the first assimilation (left), last assimilation (middle) and O-B of the two assimilations (dashed red line is first assimilation and solid red line is last assimilation), c. the same as a but for salinity and d. the same as b but for salinity.

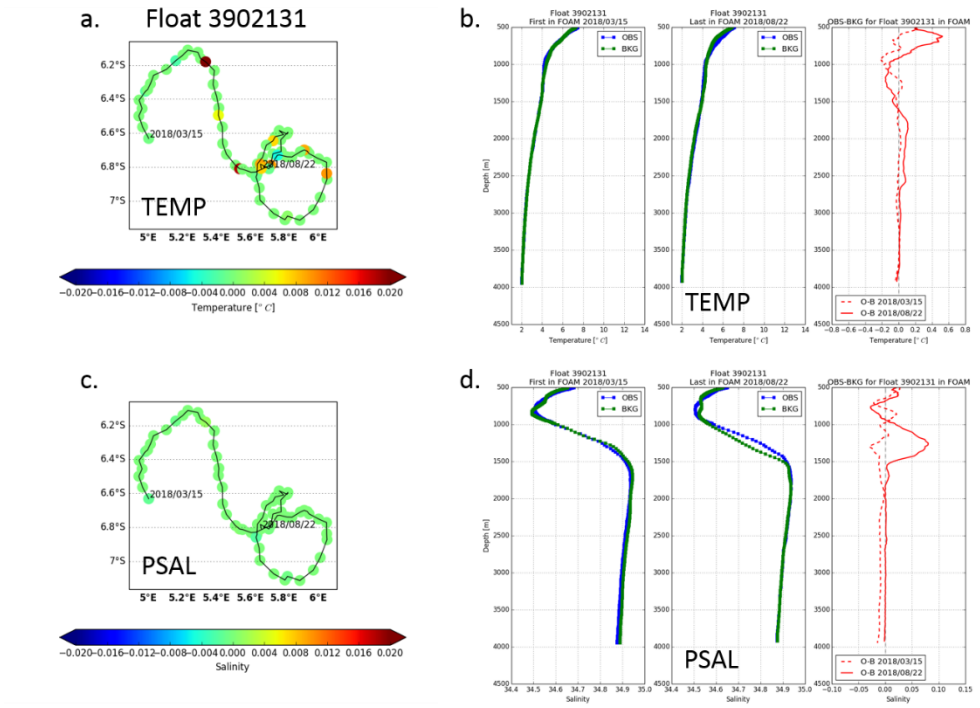

Figure 6. Trajectory and profiles for Float 3902131: a. temperature profile trajectory with colour indicating the average observation-minus-background (O-B) for depths below 3000 m, b. temperature observation (blue) and model background (green) profiles for the first assimilation (left), last assimilation (middle) and O-B of the two assimilations (dashed red line is first assimilation and solid red line is last assimilation), c. the same as a but for salinity and d. the same as b but for salinity.

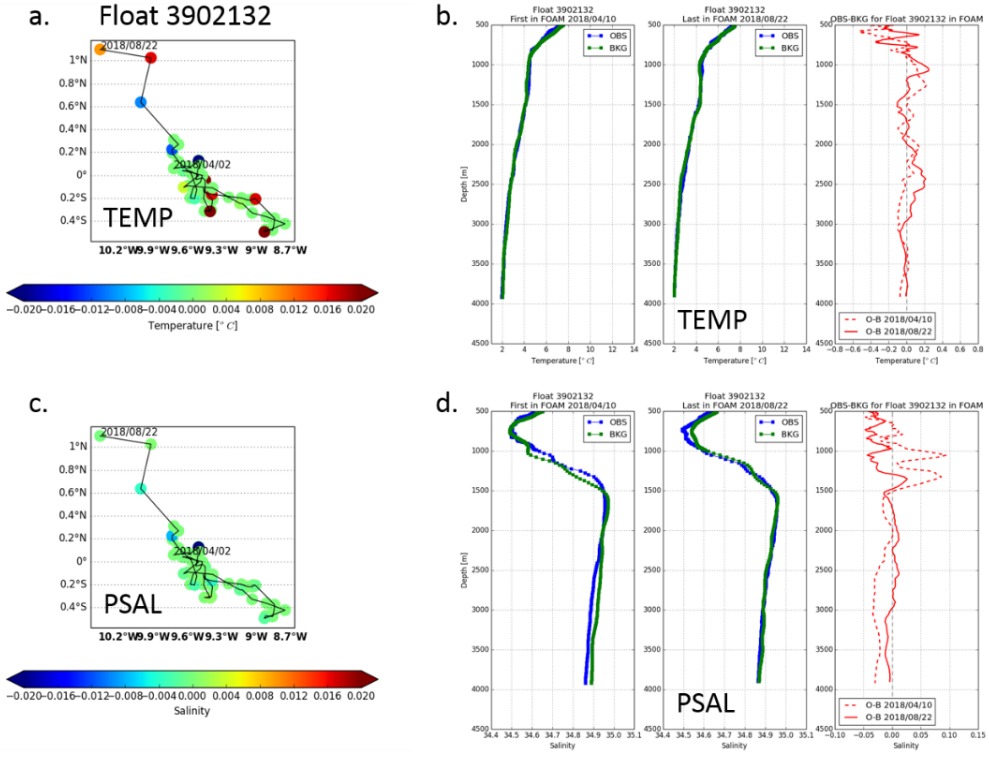

Figure 7. Trajectory and profiles for Float 3902132: a. temperature profile trajectory with colour indicating the average observation-minus-background (O-B) for depths below 3000 m, b. temperature observation (blue) and model background (green) profiles for the first assimilation (left), last assimilation (middle) and O-B of the two assimilations (dashed red line is first assimilation and solid red line is last assimilation), c. the same as a but for salinity and d. the same as b but for salinity.

2.3 Impact of drifter observations

2.3.1 Experimental set-up

Using the ocean forecasting system as described above, a control experiment was run along with two additional experiments with-holding 20% and 50% of the available drifters on each day. All experiments were run for 1 month (03 July – 3 August 2018) and used the same inputs (observations, surface forcing, etc.) with only the fraction of drifter observations varying between experiments. The surface fluxes were taken from our operational NWP system and observations extracted from our observation database with a cut-off applied to ensure only those observations which would have been available in near-real time were extracted.

An example of the spatial coverage of drifter temperature observations over a single day is shown in Figure 8. It is apparent that the coverage is significantly lower in the equatorial regions, particularly the equatorial Pacific, and near the polar ice edge.

2.3.2 Impact

In a single assimilation cycle in the Met Office global system, there are approximately 2 million SST observations, primarily from satellites, with approximately 35 thousand SST observations from drifters (<2%). If all SST observations were unbiased, the impact of the drifter observations alone would be limited. There may be localised impacts at high latitudes and where clouds limit the satellite coverage. However, the main impact of drifter observations in our system comes from their use as unbiased reference observations in our bias correction scheme.

The baseline SST RMSE in our control experiment, estimated from all observations, is shown in Figure 9. This shows that, as expected, there are higher RMS errors in the most dynamic regions such as the Western Boundary Currents (WBCs) and the Antarctic Circumpolar Current (ACC), with lower values at mid-latitudes in the centre of each ocean basin. However, the distribution of drifter observations is such that these high variability regions are relatively under-sampled (see Figure 8, lower panel).

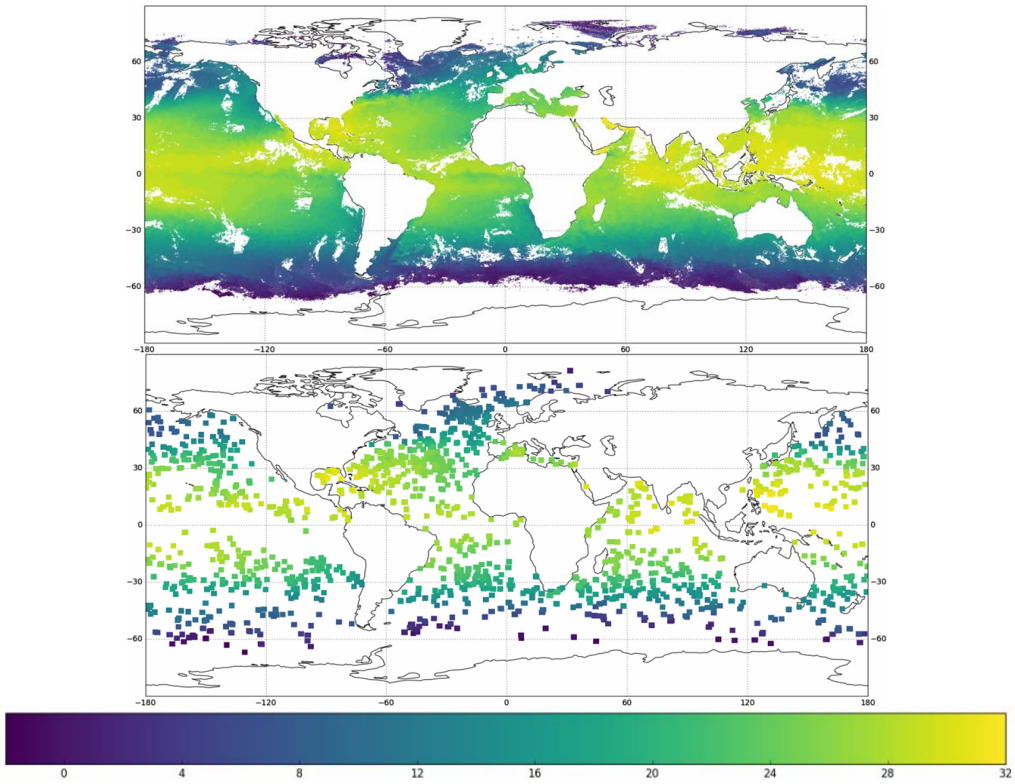

Figure 8: All available SST observations assimilated into the Met Office global ocean forecasting system on 03-Jul-2018 (top) and the global network of drifter temperature observations on the same day (bottom).

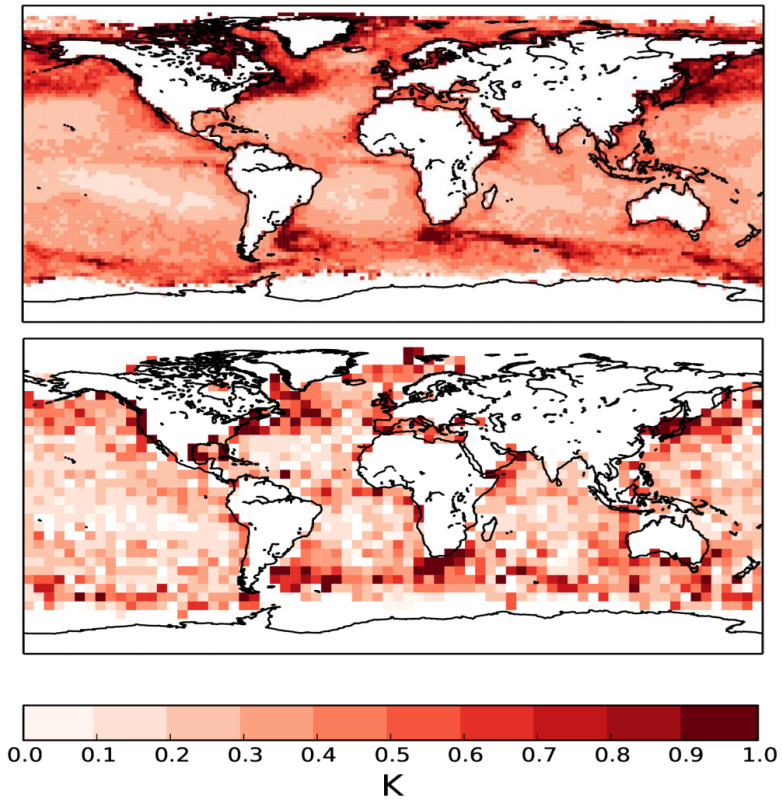

Figure 9: SST (top) and upper 5m temperature profile (bottom) innovation RMS errors from the control experiment using all available observations over the 1-month experiment. Values have been averaged in 1x1 degree bins for SST and 5x5 degree bins for profile observations

By with-holding a fraction of the available drifters, we expect to reduce the efficacy of the bias correction and so increase the SST RMSE. In the experiment where we remove 20% of the available drifters, there is a modest but widespread degradation in the SST RMSE (Figure 10, upper panel). When we with-hold 50% of the drifters (Figure 10, lower panel) from the bias correction and assimilation, the impact is substantial, but still patchy.

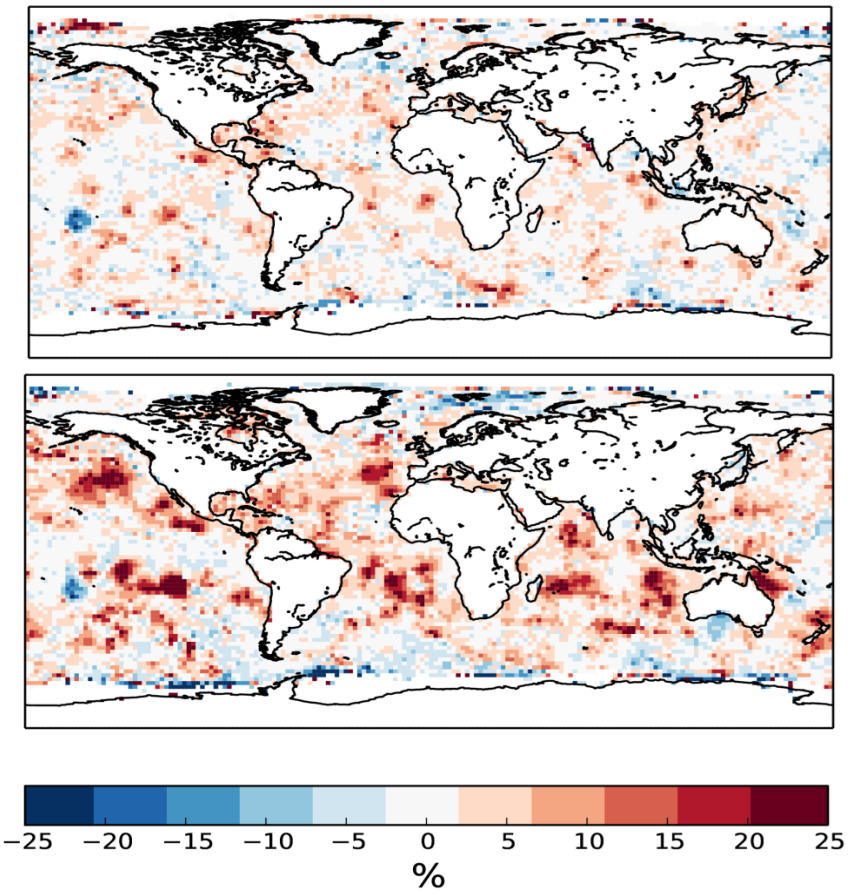

Figure 10: Percentage change in SST innovation RMS errors from the control experiment to the experiment with-holding 20% (top) and 50% of drifters (bottom). Values have been averaged in 1x1 degree bins. Red regions indicate an increase in the RMSE.

Since the SST RMSE is estimated using the bias-corrected SST observations, this analysis is not independent of the effect of the drifters on the bias correction itself. Therefore, we have also used the observations in the upper 5m of the ocean from temperature profiles to provide an independent confirmation of the impact of with-holding drifters from our assimilation and bias correction system. Although there are many fewer upper ocean temperature profile measurements than SST observations, Figure 9 shows that the variability sampled by these observations is very similar to that sampled by SST observations. The impact of removing 20% and 50% of drifters (Figure 11) is spatially similar to that seen when using the bias corrected SST observations, but with in situ profile observations (which are independent of the bias correction scheme), the RMSE changes by more than 50% in some regions. Although there are localised regions where the RMSE decreases when removing drifter observations, on average there is a substantial degradation due to the removal of drifter observations.

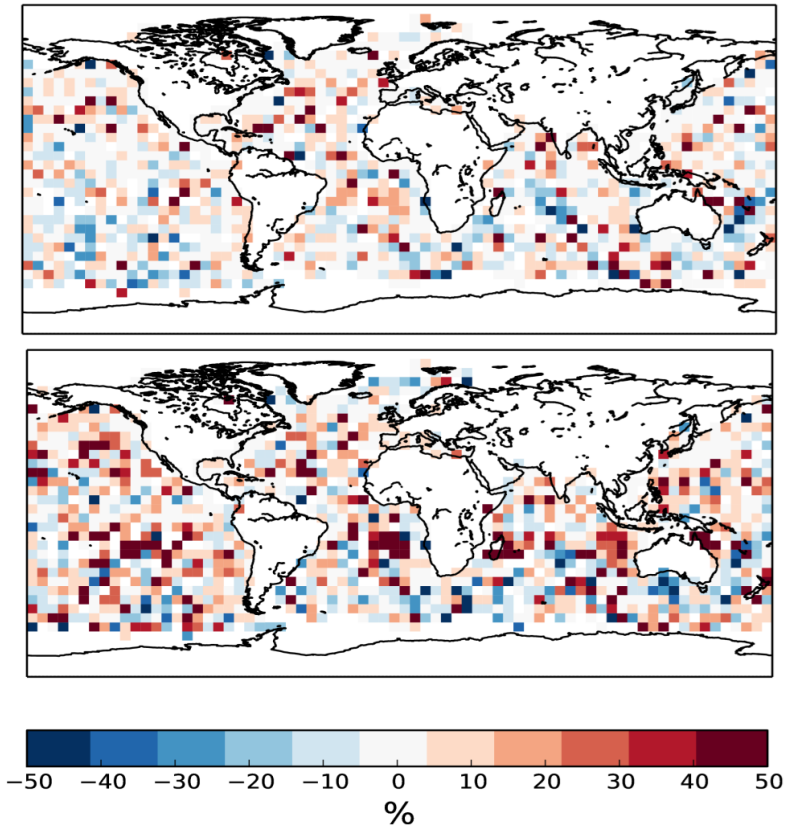

Figure 11: Percentage change in upper 5m temperature profile innovation RMS errors from the control experiment to the experiment with-holding 20% (top) and 50% of drifters (bottom). Values have been averaged in 5x5 degree bins. Red regions indicate an increase in the RMSE.

The pattern of regions of RMSE degradation when removing drifters may be a result of the drifters being caught in eddies repeatedly sampling the same ocean region. The removal of these then leaves no in situ observations to update the bias correction in that region.

In both experiments we see little impact from removing drifters in the equatorial regions, particularly the equatorial Pacific. This clearly correlates with the location of drifters. The impact of removing drifters elsewhere suggests that we could decrease the SST RMSE in the equatorial regions if we had suitable in situ observations to use within the bias correction scheme. Similarly, at high latitudes there appears to be a small improvement in the SST RMSE when 50% of drifters are removed. This is a region with few satellite or in situ observations and so there may be deficiencies in the bias correction scheme here, or there may be biases in the drifter observations themselves.

2.4 Conclusion

The number of Deep Argo floats is still very small compared to the Core Argo floats. This handful of measurements of temperature and salinity in the deep ocean has a positive impact on the performance of FOAM, especially for depths deeper than 2000 m. Even with only a few profiles assimilated into the model over a month, there is an improvement in the estimate of temperature and salinity in the deep ocean (e.g. Float 6901601), when comparing the first and last time the profile being assimilated. It would be interesting to investigate the impact of Deep Argo floats in other ocean basins and their impact on ocean heat content. Given the positive impact of a limited number of Deep Argo floats, more Deep Argo would bring more benefits to the development of ocean model.

While the removal of 20% of drifters results in a modest impact on the short-range SST and upper ocean temperature forecast errors, removing half of all drifters causes an increase in the upper ocean temperature RMSE by >20% across a large fraction of the global ocean, focussed on the mid latitudes where there are a significant number of existing drifters. It is worth noting that the impact may be larger than estimated using these short experiments, as the full effects may become apparent over seasonal time-scales. The equatorial and WBC regions which are under-sampled by the existing drifter network do not show a significant impact from the removal of half of the existing observations, but improved sampling is likely to improve the bias correction and reduce innovation errors in these high variability regions.

3 Impact of AtlantOS network in the Mercator Ocean global analysis and forecasting system

This study specifically tackles the question of the potential contribution of surface drifting buoys and deep Argo pilot arrays, which are generally not assimilated in the Mercator Ocean systems. Thus, the present work plans to provide quantitative elements for defining the strategy of the future assimilation of these *in situ* networks in the global Mercator Ocean system operated in near real-time by the Copernicus Marine Environment Monitoring Service (CMEMS) since 19 October 2016.
The spread of the four Global Reanalysis Ensemble Project (GREP) reanalysis is used to quantitatively and regionally characterize temperature and salinity uncertainties. Then, we investigate the consistency of the current operational system with regard to these independent data sets (not yet assimilated). Finally, numerical experiments quantify the impact of assimilating these observations using the experimental system.

3.1 Data and methodology

Two Mercator-Ocean systems have been used in this study. As mentioned previously, the 1/12° operational system has been compared with the *in situ* networks in order to examine the differences of the operational solution with these independent observations. The ¼ experimental system has been used to assess the contribution of the *in situ* networks by comparing numerical simulation, with and without the assimilation of each *in situ* network.

3.1.1 The 1/12° Operational System

The global high resolution monitoring and forecasting system PSY4V3R1 is based on version 3.1 of the NEMO ocean model (Madec and the NEMO team, 2008), which uses a 1/12° ORCA grid type (with a horizontal resolution of 9 km at the equator, 7 km at mid-latitudes and 2 km near the poles). The water column is discretisized into 50 vertical levels, including 22 levels within the upper 100 m, with 1-m resolution at the surface and 450m resolution at the bottom. The bathymetry is a combination of interpolated ETOPO1 (Amante and Eakins, 2009) and GEBCO8 (Becker et al., 2009) databases. The PSY4V3R1 system was initialized on 11 October 2006, based on the temperature and salinity profiles from the EN4 monthly gridded climatology (Good et al., 2013), averaged for the period October–December 2006. Assuming that the velocity field is zero at the start, the model physics then spins up a velocity field in balance with the density field. More details about the spin-up procedures can be found in Lellouche et al. (2018). The atmospheric fields, which force the ocean model, are obtained from the European Centre for Medium-Range Weather Forecasts-Integrated Forecast System (ECMWF-IFS) at 3-hr resolution, in order to reproduce the diurnal cycle. A mean dynamic topography (MDT), based on the "CNES-CLS13" MDT and taking into account the EGM-DIR R4 model of the GOCE geoid and observation innovations in reanalysis, has been used (Rio et al., 2014). More details concerning parameterization of the terms included in the momentum, heat and freshwater balances (i.e., advection, diffusion, mixing or surface flux) or MDT procedures can be found in Lellouche et al. (2018).

3.1.2 The ¼° Experimental System

The global experimental system used to perform OSSEs is based on the version 3.1 of the NEMO ocean model, which uses a 1/4° ORCA grid type (horizontal resolution of 27 km at the equator, 21 km at mid-latitudes and 6 km poleward. The atmospheric fields, which force the ocean model, are obtained from the European Centre for Medium-Range Weather Forecasts-Integrated Forecast System (ECMWF-IFS) at 3-hr resolution. More details concerning parameterization of the terms included in the momentum, heat and freshwater balances (i.e, advection, diffusion, mixing or surface flux) can be found in Lellouche et al. (2013). In addition to the ocean model, data assimilation procedures based on a reduced-order Kalman filter derived from a SEEK filter (SAM2, Brasseur and Verron 2006) are used for the assimilation of satellite and *in situ* observations. A correction for the slowly evolving large-scale error of the model in temperature and salinity is applied. More details in the data assimilation procedures can be found in Lellouche et al. (2013).

3.1.3 The in situ networks

The integration of *in situ* observations depends on several steps from the data collection to the recovered data at Mercator Ocean. In situ data, in Real Time and delayed time, are coming from the CORIOLIS data center. It collects the data on global networks (GTS , ARGO/GOSUD/OceanSITES GDACS) as well as regional data centers, quality controls them and makes them available on a daily basis to the operational and research community.

From this data set, a subsampling is applied to fit the data sets to the resolution of Mercator Ocean systems. Basically, this subsampling consists in only keeping one profile (T and/or S) for a given instrument per 24h and per 0.1° x 0.1° square (with several criteria selecting the "best" profile). During these different steps of integration, the number of qualified data to be assimilated can significantly change.

3.1.4 The global surface drifter network

The global drifter array is composed of around 1200-1400 surface drifting buoys, which are deployed globally (Lumpkin et al., 2017) and transmit hourly data. However, due to the equatorial divergence at the surface, important gaps are found in the three equatorial oceans (Figure 12). For several reasons, the number of recovered data at Mercator Ocean is not constant, and jumps in the number of recovered data exist. In addition, criteria of subsampling from CLS involve that most of the selected measurements (1 per day, per 0.1x0.1 square) are from the first hour in UTC time (Figure 12), and this could lead to bias in the solution. The transmission process from the acquisition to the integration to the operational system needs to be continuously verified to insure the best use of observations in operational systems. Because surface drifting buoys have not systematic pressure sensor, the depth of the measurement is set to a standard value (with a standard depth of 0.5 m), making impossible to determine the depth of the measurement. For that reason, this dataset is not assimilated in the current operational system.

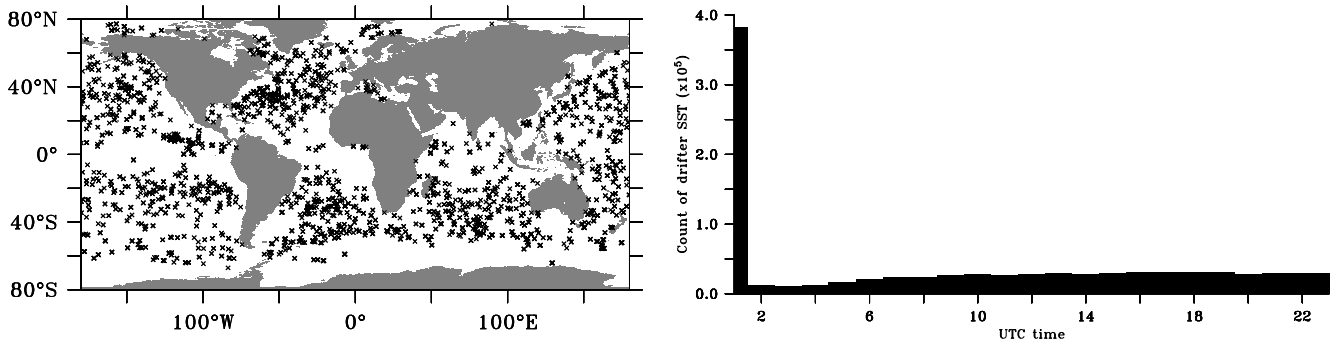

Figure 12: (left panel) Locations of surface drifting buoys the 15th October 2016. (right panel). Time of the day (in UTC time) of the selected measurement per 0.1°x0.1° grid per day for the year 2016.

3.1.5 The Deep Argo pilot arrays

The deep Argo pilot arrays have started at the beginning of 2016, with an increase of around 60 active floats in 2018 (Figure 2), and consist in several experimental deployments, which are mostly used for technological development (e.g., sensor calibration, uncertainty assessment, prototype test). In addition to these technical purposes, the location of these pilot arrays has been also chosen for scientific objectives, including monitoring deep ocean warming (Figure 13). It is noteworthy that these pilot experiments are also used to define standard characteristics of deep floats (e.g., cycle time, parking depth, vertical resolution), and thus, the available floats sample at different time interval, drift at different parking depth, and can have different vertical resolution (Zilberman and Maze, 2015). During this pilot phase, some issues have been revealed on the CTD pump, especially for pressure and salinity sensor (e.g., Le Reste et al., 2016), making the quality control at 2 (probably good data) for temperature, and 3 (bad data that is potentially correctable) for salinity below 2000 dbar. Similarly to the surface drifting buoys, the deep Argo profiles from these pilot experiments are not assimilated in the current Mercator Ocean operational system.

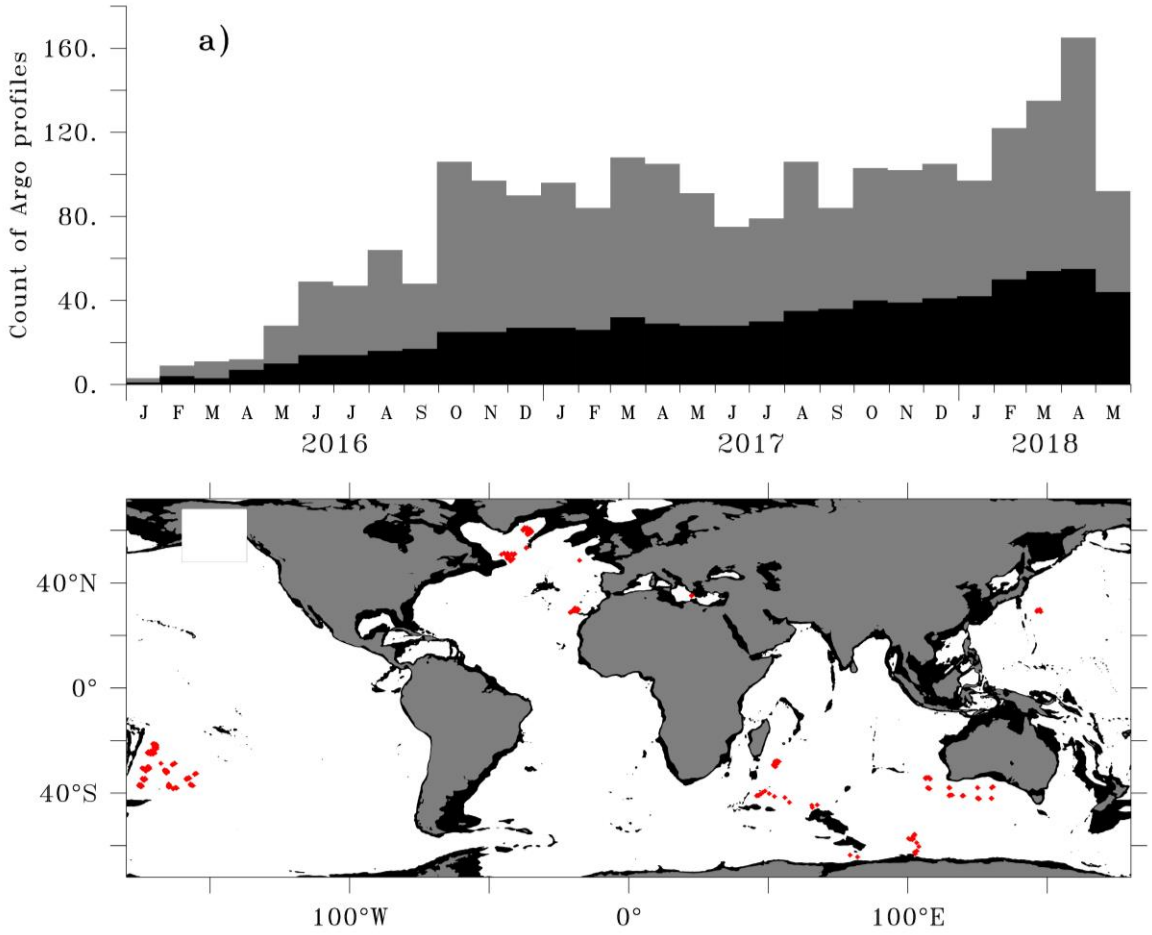

Figure 13: (upper panel) Count of deep Argo profiles (grey) and deep Argo floats (black) for each month from January 2016 to May 2018. (lower panel) Locations of the deep Argo profiles from the pilot arrays in 2016.

3.2 The surface drifting buoys

In order to investigate the uncertainty on the representation of SST in monitoring and analysis system, the standard deviation of SST of the four GREP reanalysis is time-averaged during the 2016 year (Figure 14). The strongest differences (>1°C) in the GREP reanalyses are preferentially found in the high-variability

regions, such as the western boundary current (WBC) and frontal zones of the Southern Ocean. The amplitude of difference is much lower in low-latitudes regions (around 0.1-0.2°C).

In addition to the spread of the GREP product in representing SST, Figure 14 shows the SST difference between drifters and the daily fields of the operational system (no drifter assimilation). The patterns are similar to the spread of the GREP product, with higher amplitude in high-variability regions (>1.4°C). The main difference is mostly due to the high-frequency variability, which has been filtered in the monthly fields of GREP. Thus, this shows that SST uncertainty and drifter/operational system inconsistency have similar patterns and similar amplitude, providing regions where efforts should be preferentially done.

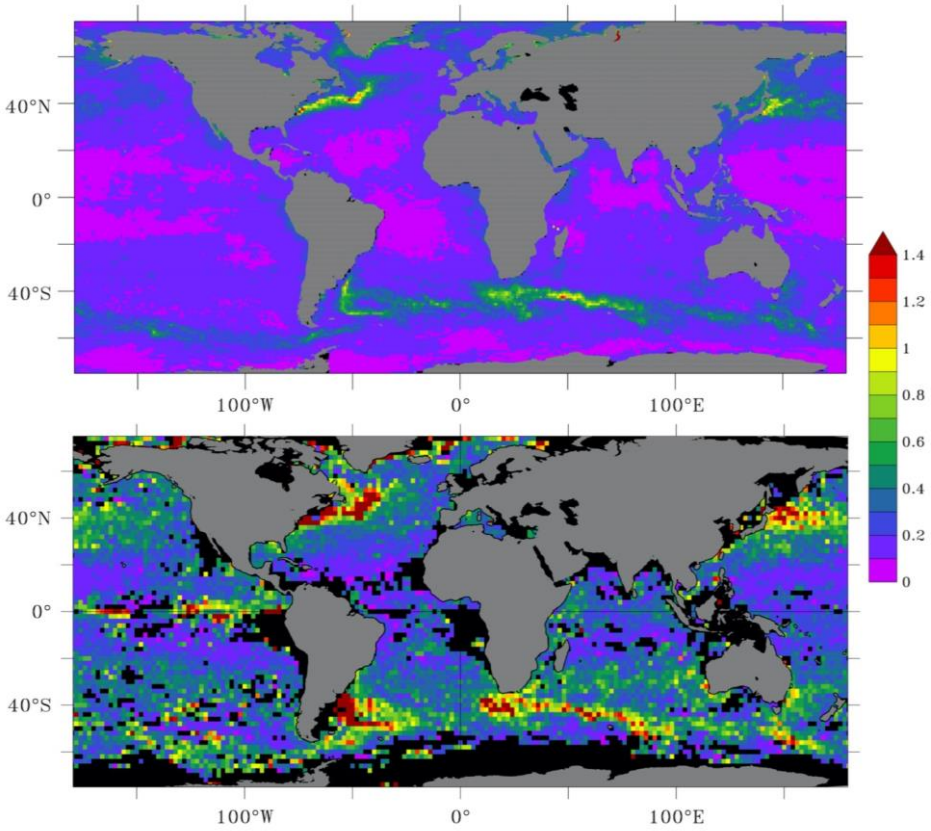

Figure 14: (Upper panel) Time-averaged of monthly standard deviation of SST from the four members of the GREP ensemble for the year 2016. (Lower panel) 2°x2° bin-averaged daily RMS difference in SST between drifters and the operational system for 2016. The operational system values have been obtained by subsampling in space and time of the drifter locations. Unit is °C.

3.2.1 Contribution of the drifter array in the OSE

In order to quantify the consequences of assimilating the global drifter array, two simulations have been performed for the year 2016 using the experimental system described above. The CONTROL run includes the assimilation of satellite observations (i.e., altimetry and SST) plus Argo observations. The ADD_DRIFTER run corresponds to the same simulation to the CONTROL run, but with the assimilation of drifter observations additionally. The question is how additional drifter observations impact on the solution.

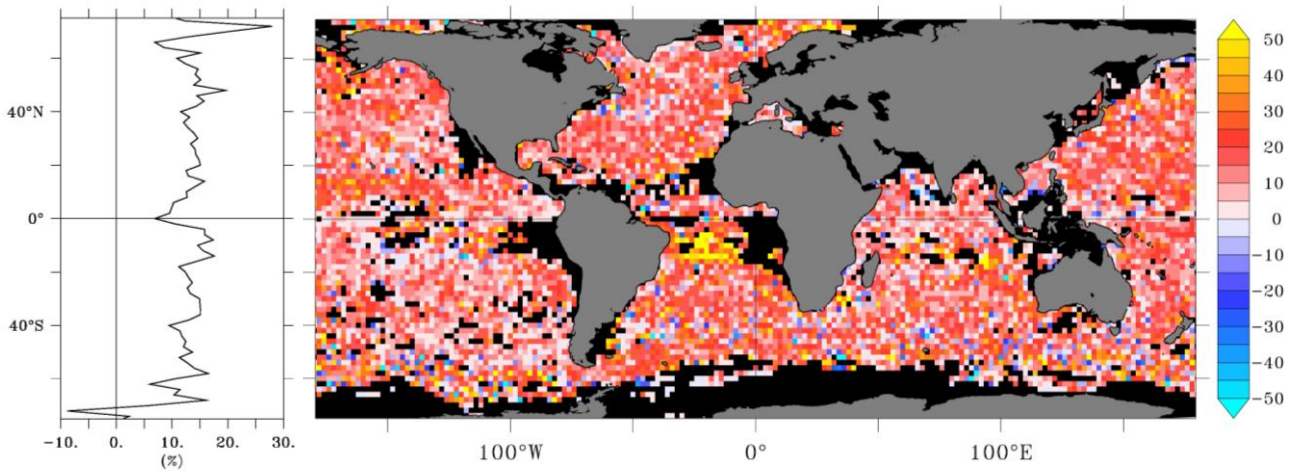

Figure 15: Reduction of RMS difference (in %, 2°x2° bin-averaged) from the CONTROL run to the ADD_DRIFTER run compared with drifter values ((left panel) spatial map, (right panel) zonally averaged). The run values have been obtained by subsampling in space and time of the drifter locations. Unit is percent.

In Figure 15, the reduction of RMS difference from the CONTROL run to the ADD_DRIFTER run compared with drifter values demonstrates that the assimilation of drifter reduces differences with drifter values at drifter locations. In general, RMS difference is reduces, with values exceeding locally 50% in the tropical Atlantic. The zonally averaged RMS difference reduction is around 10-15% when drifters are assimilated. The same approach is done at the Argo locations to investigate whether drifter assimilation will reduce the RMS difference between simulations and Argo values in the upper 5m, but results indicate that the reduction is not significant (~1%, not shown).

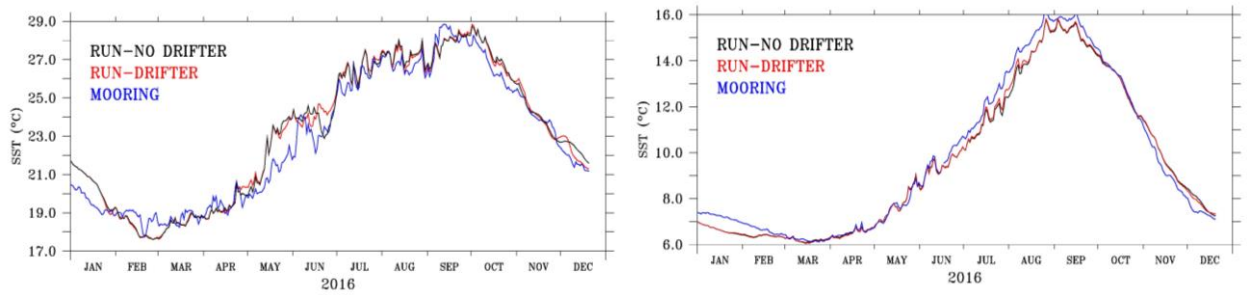

Figure 16: Mooring SST (blue) and SST from the CONTROL run (black) and ADD_DRIFTER runs (red) at (left panel) 145E, 32N and (right panel) 145W, 50N. Mooring data are from Ocean Climate Stations, at the PAPA and KEO stations (https://www.pmel.noaa.gov/ocs/). Unit is °C.

In order to compare with independent data set, SST from the two simulations is shown at the location of two moorings in the Kuroshio and in the North Pacific gyre (Figure 16). In general, ADD_DRIFTER is more consistent with mooring data, the RMS difference is slightly decreased when drifter are added in the observing system. At the PAPA station, the RMS difference decreases from 0.43 to 0.38°C, and at the KEO station, from 0.77 to 0.75°C. This demonstrates that the addition of drifters can lead to significant improvement of the SST representation.

Thus, the assimilation of the current drifters appears to improve the analysis system at (i) at the drifter locations, (iii) at some mooring locations and, (ii) negligible at the Argo locations. In any case, it does not seem to degrade the solution, and further investigations are required to optimize the use and integration of the drifter measurements. As mentioned previously, the subsampling of the drifter data can cause some bias due to the selected profile, it might be of interest to get some averaging, or add more profiles during the day. In addition, due to the important changes in the number of recovered data, it is important to

systematically check the quantity of recovered data, allowing preventing important gaps in the assimilated data. Specific work is also needed to analyze the consistency between *in situ* and satellite SST. This is also important to perform longer experiment in order to investigate the contribution of the global drifter array on interannual and longer time scales. The present work has to be seen as a first step toward a better integration of drifter observations in ocean operational systems.

3.3 The deep Argo floats from the pilot array

Unlike the upper ocean, the deep ocean (below 2000 dbar) is not regularly sampled at global scale, and is limited to sparse hydrographic sections repeated every decade and short-lived moored arrays of confined spatial coverage. Without data assimilation, ocean reanalyses are almost not constrained at these depths, and the spread of analysis fields among the GREP reanalyses is a good indicator of uncertainty and the need for more intensive sampling in the deep ocean.
In order to illustrate the uncertainty of the ocean reanalyses, the 3000m-temperature and -salinity standard deviations from the four GREP reanalyses are basin-averaged in Figure 17.

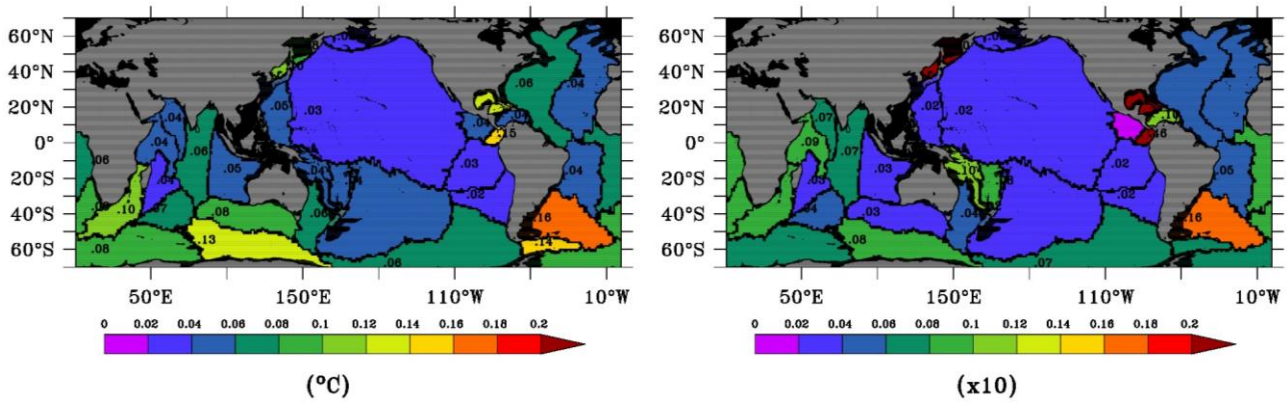

Figure 17: Basin-averaged 3000m-temperature standard deviation for the year 2016 from the GREP reanalyses for (left panel) temperature and (right panel) salinity. Standard deviation, with amplitude higher than 0.02 indicated in black. Unit is °C for temperature.

The spread of the reanalysis fields show regional patterns, with higher amplitude in the region of the Brazilian current, and to a lesser extent in the Southern Ocean (around 0.1°C for temperature and 0.01 for salinity). In general, regional patterns of temperature and salinity spreads are consistent.

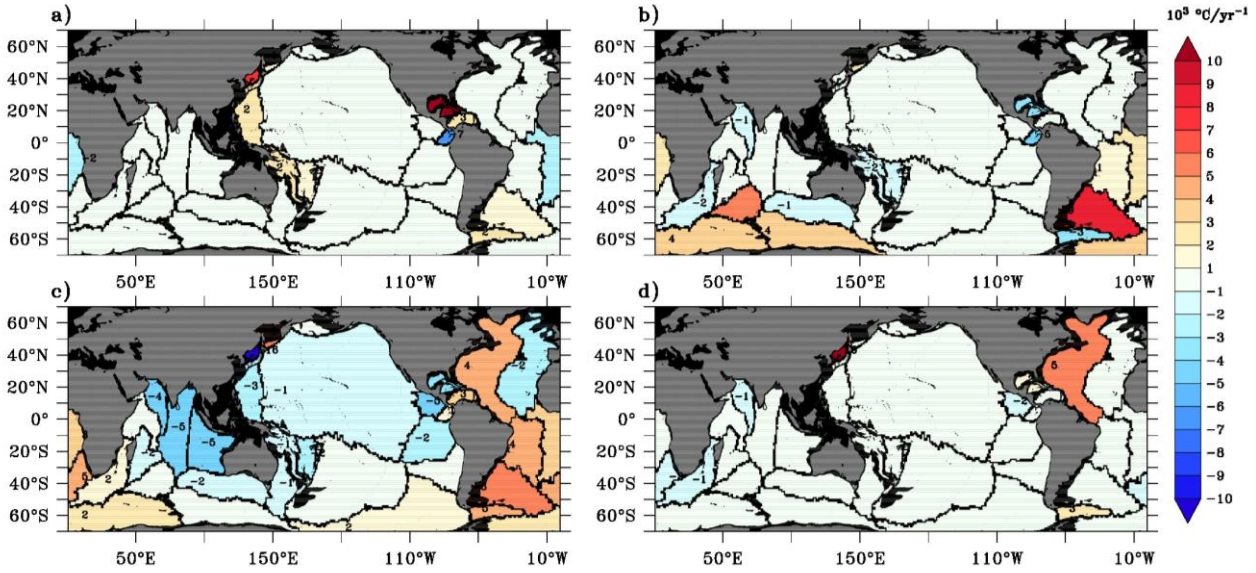

Figure 18: Basin-averaged 3000m-temperature trend for the period 1993-2017 from (a) C-GLORS, (b) FOAM, (c) GLORYS2V4 and (d) ORAS5. Temperature trend, with amplitude higher than 1 are indicated in black. Units is 103 °C/yr.

Another interesting point of the GREP product concerns the spread of the long-term temperature trends. In Figure 18, the four reanalysis show strong differences in the representation of the 1993-2017 temperature long-term trend at 3000m. C-GLORS and ORAS5 do not show significant temperature changes on the 1993-2017 period, while FOAM and GLORYS2V4 show stronger temperature changes, which are more consistent with literature in terms of magnitude and regional distribution (Purkey and Johnson, 2010; Kouketsu et al., 2011; Desbruyeres et al., 2016). Thus, this analysis illustrates the amplitude of errors in the deep ocean.

As for the global drifter array, measurements below 2000 dbar from the deep Argo pilot arrays are not assimilated in the current operational system (See Section 2.2), and it is of interest to evaluate the amplitude differences of the operational system with regard to these observations. In Figure 19, the operational system has been subsampled in space and time of the location of a deep Argo float deployed in March 2017 (WMO 4902324) in the North Atlantic around 26°N, and compared to the temperature from the deep Argo float for the period March 2017 to June 2017. The “operational system minus deep float” difference indicates that model bias dominates (±0.1°C). Similarly, the RMS differences of temperature and salinity has been estimated by co-located the daily of the operational system to the 2313 deep Argo profiles (period Jan 2016-May 2018, Figure 20). Consistently with the spread of the GREP reanalyses, the RMS difference is around 0.1°C for temperature and 0.01 for salinity, illustrating the errors of the current operational system in the deep ocean, without regular global observations.

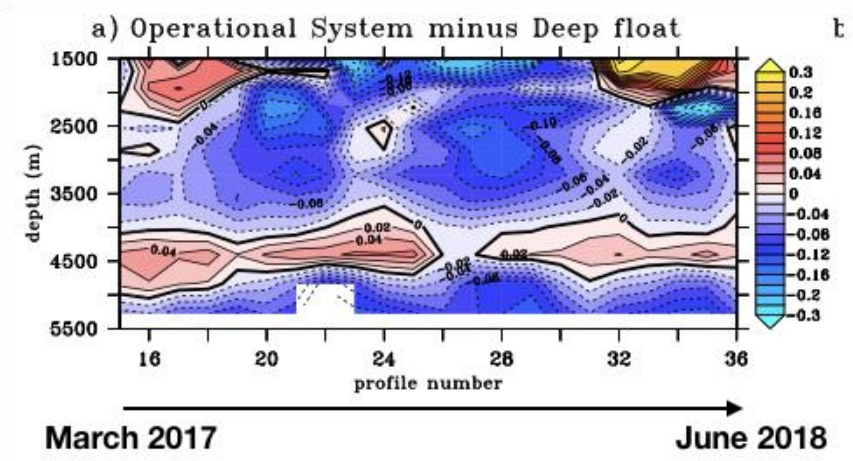

Figure 19: PSY4V3R1-minus-Deep float temperature differences from the float deployed in the North Atlantic Ocean around 26N (WMO 4902324) in March 2017. The PYS4V3R1 has been colocated in space and time to be compared with the deep pilot array. Unit is °C.

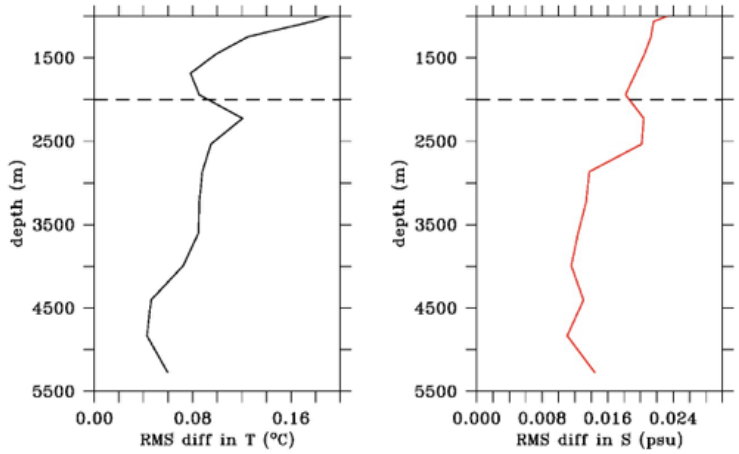

Figure 20: Global RMS differences between the PSY4V3R1 operational system and the 2313 deep Argo profiles for (a) temperature and (b) salinity. Units are °C and psu.

3.3.1 Contribution of the deep Argo in the OSE

Similarly to the drifter array, the contribution of the deep Argo pilot arrays have been examined by performing two simulations using the experimental system, with and without assimilating the deep component of the deep Argo profiles (below 2000dbar). The CONTROL run (assimilation of SST, altimetry, and core-Argo) is the same one than for the drifter experiment. This simulation is compared with the ADD_DEEP run, in which the deep Argo component of the Argo pilot array is assimilated.

In Figure 10, the bias and RMS difference for temperature and salinity have been calculated by co-locating the CONTROL and ADD_DEEP simulations to the location of a deep Argo float deployed in the North Atlantic. A net decrease of the temperature and salinity bias and RMS difference is seen when the deep Argo profile is assimilated. At 2200m, the temperature bias decreases from -0.20°C to -0.03°C, and the RMS from 0.20°C to 0.10°C, demonstrating the significant error reduction when deep floats are assimilated.

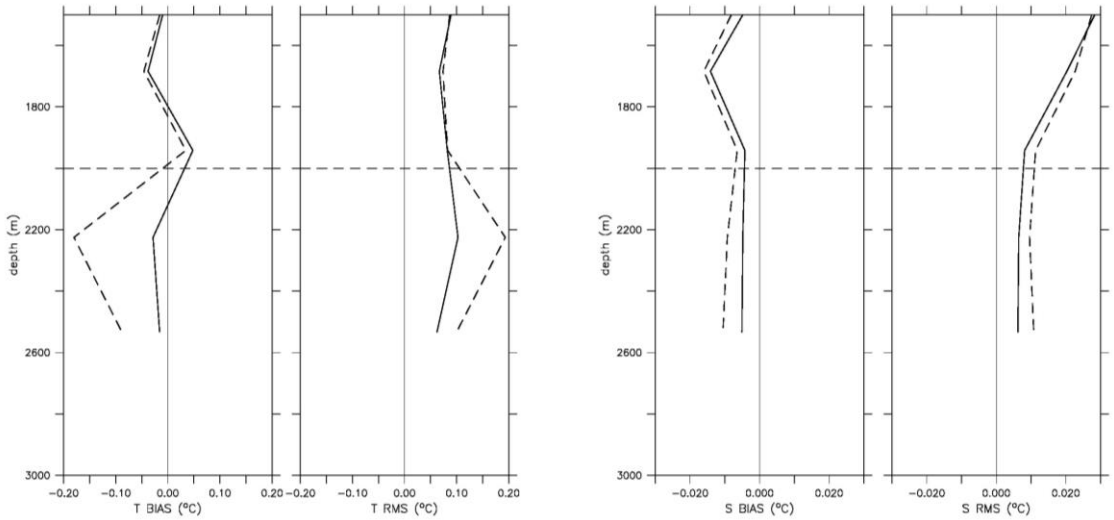

Figure 21: Bias and RMS difference for (a,b) temperature (in °C) and (c,d) salinity, of the CONTROL run (thick dashed lines) and the ADD_DEEP run (full thick lines), compared with observations from a deep Argo float (WMO 6901762). The run values have been obtained by subsampling in space and time of the deep Argo profiles locations.

In order to go further in the impact assessment, Figure 22 shows the 2300 m temperature and salinity differences (color-shading) in the North Atlantic for the period August 2016 to November 2016, in a region where the two deep floats have been deployed. The 2300m-temperature and –salinity, area-averaged in the square region, from the two simulations are compared with values from deep Argo floats (Figure 22, right panels), and show that the assimilation of the deep Argo float constrains the solution toward observations. Even if temperature estimates from the two Argo floats (around 3.0°C) are more consistent than salinity estimates, both quantities are well reproduced by the ADD_DEEP numerical simulation, compared to the CONTROL run. The assimilation of the float has a larger influence than the locations of the float, and both temperature and salinity show a southward extension along the coast in the southwest corner of the square. Further investigations would be necessary to assess the model background error variance and correlation scales at those depth that are prescribed in the assimilation scheme, both for the large scale bias correction and the localized weekly analysis.

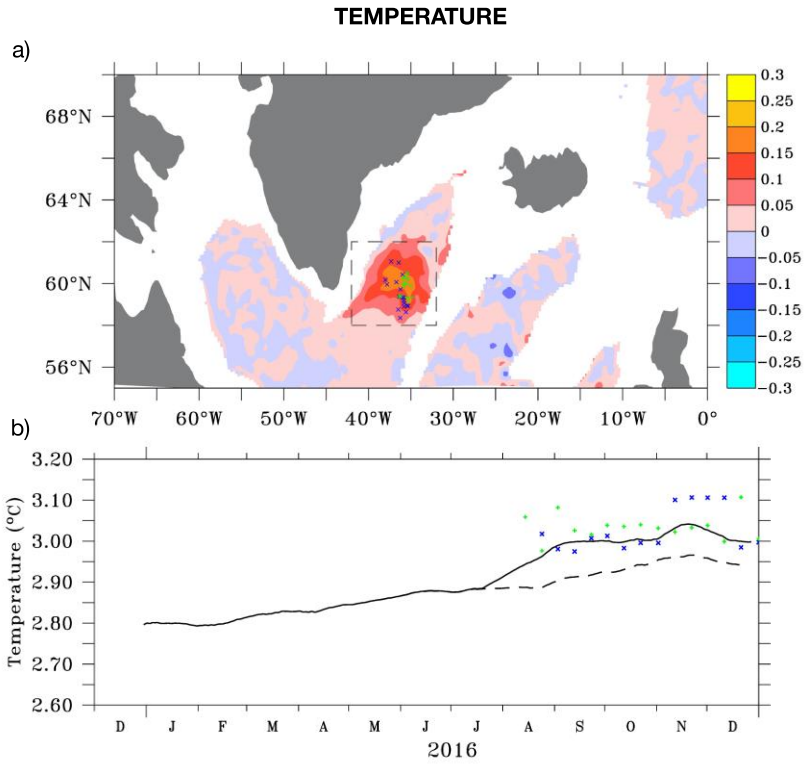

Figure 22: (a) 2300-m temperature "CONTROL-minus-ADD_DEEP" differences, averaged for the period Aug. 2016-Nov. 2016. The crosses indicate the positions of the profiles from two deep Argo profiles (WMO6901760 in blue, and WMO6901762 in green). (b) Area-averaged 2300-temperature from the CONTROL (dashed) and the ADD_DEEP (full) runs in the dashed square of right panels (42W-32W; 58N-62N). The green and blue dots indicate the observations from the two deep floats.

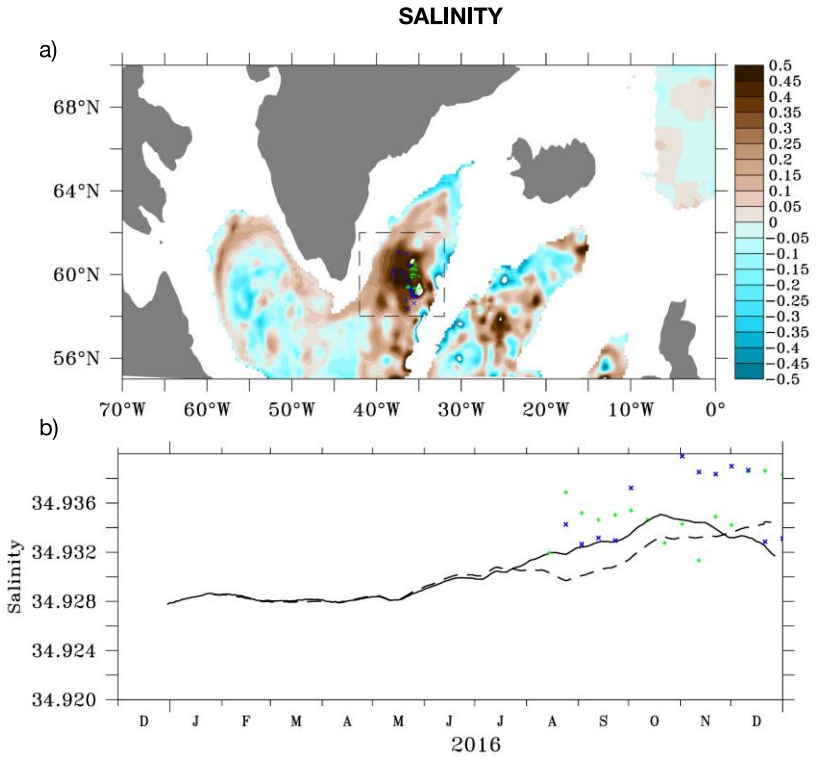

Figure 23: Same as Fig.22, but for salinity.

3.4 Conclusion

This work focusing on two observing network which are not routinely assimilated in the Mercator Ocean systems is organized in three steps. First, the uncertainties on the ocean state at the surface and at the deep ocean are evaluated using the spread of the four GREP reanalyses. Then, observations are compared to the operational system to demonstrate the necessity of the model to be constrained. Finally, dedicated experiments have been carried out, with and without the assimilation of the studied data sets.
The GREP product is useful product allowing to investigating the dispersion of four reanalyses to represent the ocean state. It is shown that at the surface, the four reanalysis have stronger discrepancies in high variability regions, such as in WBC and in the Southern Ocean. The error peaks at 1.5°C. Comparing drifter observations with the operational center show similar conclusions, confirming that errors in the operational system are consistent with the spread of the GREP product.
The integration of the drifter's observations appears to slightly benefit to the system. This is in agreement with OSSE, which have been carried out within AtlantOS in Task 1.3 (Gasparin et al., 2018). In addition, this work has highlighted that some improvements may be achieved by improving the assimilation of drifter observations, through work on the selection of the observations (subsampling) and the consistency between *in situ* and satellite observations.
The assimilation of deep Argo profiles reduces the operational minus observations difference by more than 50% at the point location. This is in agreement with results of the Task 1.3, which demonstrate that the implementation of global deep Argo array composed of 1300 floats would provide a significant constrain to the deep ocean (Gasparin et al., 2019).
It has been shown that the assimilation of the current subsampled drifter data set improves the solution, even if some refinement of the selection processes could be achieved. The deep Argo array profiles are also important to constrain the system in the deep ocean.
However, further investigations are needed to increase the benefits of assimilating these observing systems. Today, all in situ observations are almost treated in the same way in the assimilation scheme; this study will help to improve the data selection and error specification for each *in situ* individual datasets. It is also important to mention that the assimilation of new data sets, such as deep observations, will likely requires refine assimilation parameters, including tuning of the correlation scales below 2000 meter depth, more specifically in the large scale biais correction, and weight between different data sets at the surface.

4 Impact of AtlantOS in-situ observing system on ARMOR3D analysis

In this section are presented the results using the multivariate ARMOR3D data analysis system. ARMOR3D is a complementary approach to OSE studies based on data assimilation system such as the ones carried on by Mercator Océan, UK MetOffice and ECMWF. ARMOR3D is part of CMEMS Multi Observations Thematic Assembly Center (MOB TAC) and rely on the use of statistical methods to combine satellite (SLA, SST, SSS) and in-situ observations (T/S profiles) for an optimal reconstruction of global 3D temperature and salinity gridded fields.
To study the impact of the AtlantOS in-situ observing system on ocean state estimate using the ARMOR3D system, as part of task 7.4, CLS has carried on the following activities which are presented hereafter:

- Detailed inventory of the in-situ observations available in near-real-time,
- Impact of the different observing system: satellite versus in-situ,
- Impact of the Argo observing system,
- Impact of the Deep Argo observing system.

The studied period covers 1 year between August 2017 and July 2018. It has been selected very close to the date of when the analysis has been performed to benefit from the last deployments of deep Argo floats.

4.1 Inventory of the in-situ observations available in near-real-time

In-situ profiles of temperature and salinity are downloaded every day by the CMEMS MOB TAC for the operational weekly production of the ARMOR3D product. They come from CMEMS INSITU TAC which collects data from the main global networks: Argo, GOSUD, OceanSITES, GTS. The in-situ profiles are collected from product INSITU_GLO_NRT_OBSERVATIONS_013_030 which Product User Manuel is available through the following link: http://marine.copernicus.eu/documents/PUM/CMEMS-INS-PUM-013.pdf. The in-situ profiles are collected between July 2017 and August 2018 to cover the studied period plus one month before and one month after.

The in-situ observations are organised by data types (CMEMS-INS-PUM-013.pdf), which makes it easier for OSE experiments: BA data from Bathy messages on GTS, CT oceanographic CTD profiles, DB drifting buoys, MO fixed buoys or mooring time series, PF profiling floats vertical profiles, XB XBT or XCTD profiles, etc, and contain profiles or surface observations.

Between July 2017 and August 2018, 2 150 774 observation points of temperature (profiles and surface measurements) are available and 528 896 observation points of salinity (Figure 23 top). Most of the temperature observation points are limited to the surface (80 %). More than 360 000 temperature profiles and 290 000 salinity profiles are nevertheless available, among which 40 to 50% provide measurements between 1500 and 2500m depth (Figure 23 bottom). Most profiles come from Argo floats. The tropical moorings fill some gaps in the tropics and instruments mounted on sea mammals provide profiles at high latitudes of the northern and southern hemispheres.

1800 Deep Argo profiles of temperature and salinity are available for the July 2017 – August 2018 period. They are located in specific deep oceanic basins (Figure 24). These Deep Argo profiles are included in the Deep Argo experiment, and not in the Reference experiment (see the next section for the definition of the different experiments). Note that other deep profiles are also available. They come from specific cruises during which deep measurements have been made by CTD casts. Those deep profiles are included in the Reference experiment and the Deep Argo experiment.

All observation points (profiles and surface measurements):

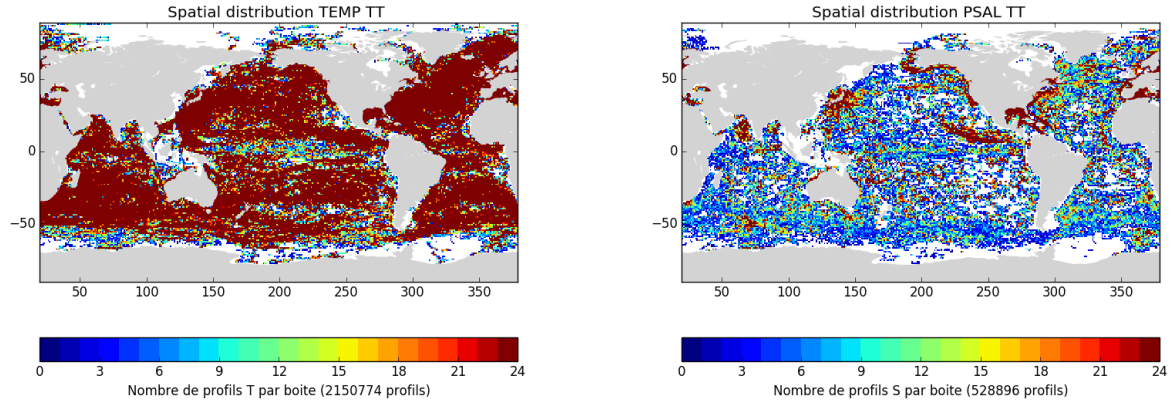

Surface observations:

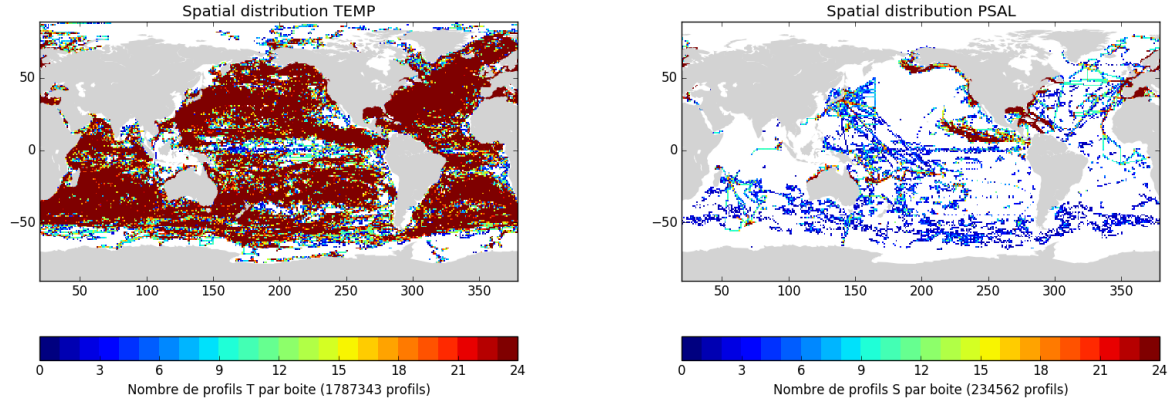

Profiles:

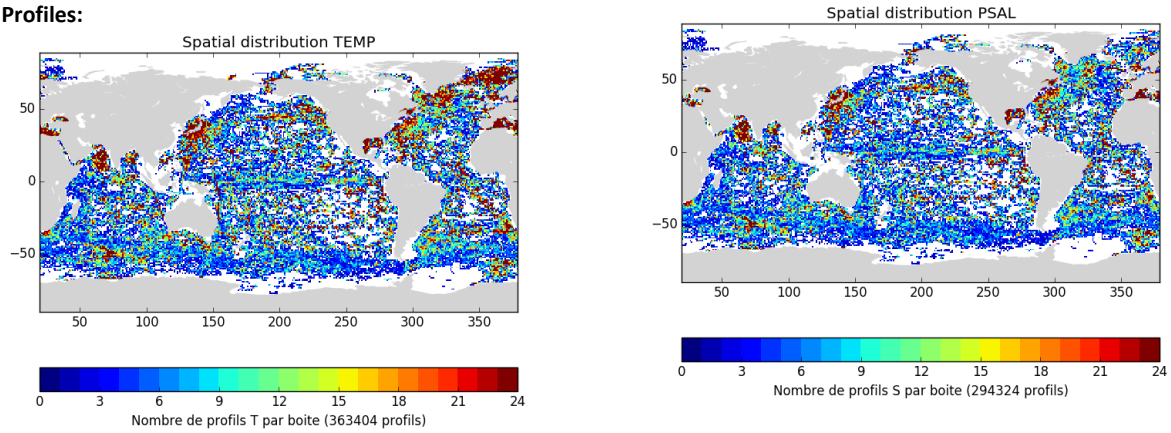

Profiles reporting measurements between 1500 and 2500m:

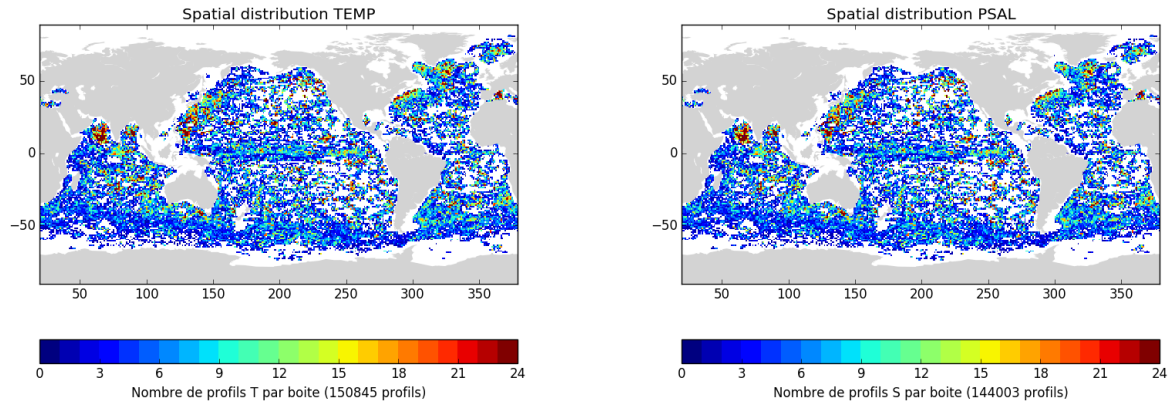

Figure 23: Spatial distribution of observation points of temperature (left) and salinity (right) for the July 2017 – August 2018 period. From top to bottom: all profiles and surface observations, surface observations only, profiles only, profiles reporting measurements between 1500 and 2500m.

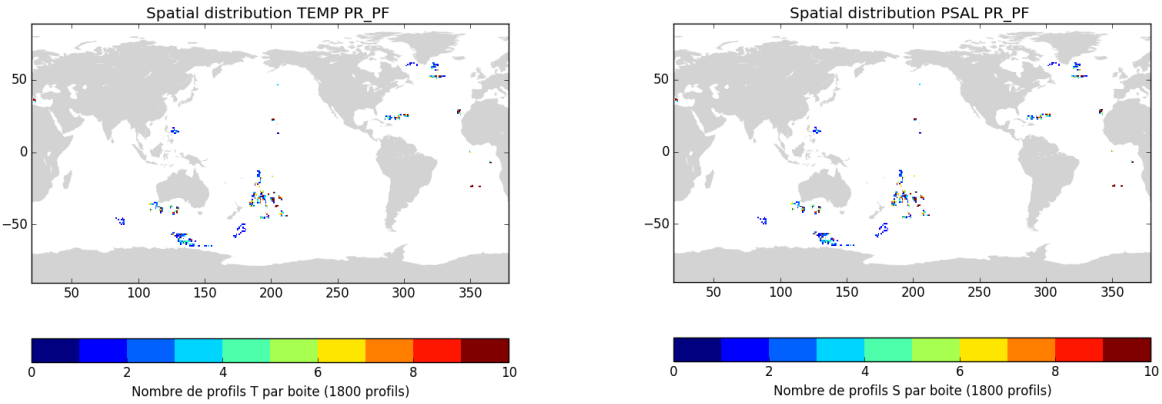

Figure 24: Spatial distribution of Deep Argo profiles of temperature (left) and salinity (right) for the July 2017 – August 2018 period.

4.2 ARMOR3D system and definition of the different experiments

ARMOR3D is part of CMEMS Multi Observations Thematic Assembly Center (MOB TAC) and rely on the use of statistical methods to combine satellite (SLA, SST, SSS) and in-situ observations (T/S profiles) for an optimal reconstruction of global 3D temperature and salinity gridded fields.
The method fully described in Guinehut et al. (2012) and recently updated in http://marine.copernicus.eu/documents/QUID/CMEMS-MOB-QUID-015-001.pdf starts from a first guess climatology (WOA13). Satellite data (SLA + SST in near-real time, SLA + SST + SSS in delayed-time) are first

projected onto the vertical using a multiple linear regression method and covariances deduced from historical observations. This step gives synthetic fields from the surface down to 1500m depth. These synthetic fields are then combined with T&S in-situ profiles using an optimal interpolation method. Analyses are performed at a weekly period on a 1/4° horizontal grid on 24 vertical levels from the surface down to 1500m depth. In a final step, the T/S fields are completed from 1500 to 5500m depth (9 additional vertical levels) with the climatology.
For the OSEs carried out during the study, the different ingredients of the ARMOR3D system are strictly identical to those used by the operational ARMOR3D chain. They are detailed in: CMEMS-MOB-QUID-015-001.pdf. Three experiments have been carried out. The synthetic fields are strictly identical in the three experiments. They differ only by the T&S in-situ profiles used in the optimal interpolation method:

- The **Reference experiment** uses all available T&S in-situ profiles as described in section 4.1, less the Deep Argo floats.
- The **No Argo experiment** uses the same T&S in-situ profiles as the Reference experiment less the Argo floats (type PR_PF of product INSITU_GLO_NRT_OBSERVATIONS_013_030).
- The **Deep Argo experiment** uses the same T&S in-situ profiles as the Reference experiment plus the Deep Argo floats (Figure 24).

4.3 Impact of the different observing systems: satellite versus in-situ

The impact of the satellite and in-situ observing systems is first studied in the Reference experiment. The Reference experiment uses all available T&S in-situ profiles as described in section 4.1, minus the Deep Argo floats. The ARMOR3D method is a two steps method which uses first the satellite observations to obtain the synthetic fields and then the in-situ observations to obtain the combined fields. During step1, the satellite observations provide the mesoscale part of the signal and during step2, the in-situ observations correct the large-scale bias that might have been introduced during step1. The impact of the two observing systems is first studied by comparing results from the first guess (WOA13), the synthetic (step1) and the combined (step2) fields and using classical residual analysis with respect to T&S in-situ observations. It is then studied by looking at Degree of Freedom of Signal (DFS) diagnostics.

4.3.1 Comparison to in-situ observations

As already mentioned, during step1, the satellite observations provide the mesoscale part of the signal. This is illustrated on Figure 25 for the temperature field at 100 m of the 16th of August 2017. Compared to the use of climatological estimates, at global scale, results indicate that 30% to 50% of the temperature fields at depth can be reconstructed from altimeter and SST satellite observations and a statistical method (compare red and blue curves on Figure 26 left). For salinity, only about 10% to 30% of the salinity can be reconstructed from altimeter observations (compare red and blue curves on Figure 26 right). Both for the temperature and the salinity synthetic fields, bias exist when compared to collocated in-situ T/S profiles (see the blue dotted lines on Figure 26).
During step2 of the ARMOR3D method, the in-situ observations are introduced in the optimal interpolation method to correct the large-scale bias that might have been introduced during step1. This is again illustrated on Figure 25 for the temperature field at 100 m of the 16th of August 2017. Comparisons of the combined fields with collocated in-situ T/S profiles are also available even if those comparisons are not independent since the in-situ observations have been used to create the fields. These comparisons are nevertheless very useful, first to check that the in-situ observations have been taken into account correctly in the method and then, to have an estimation of the residual error.

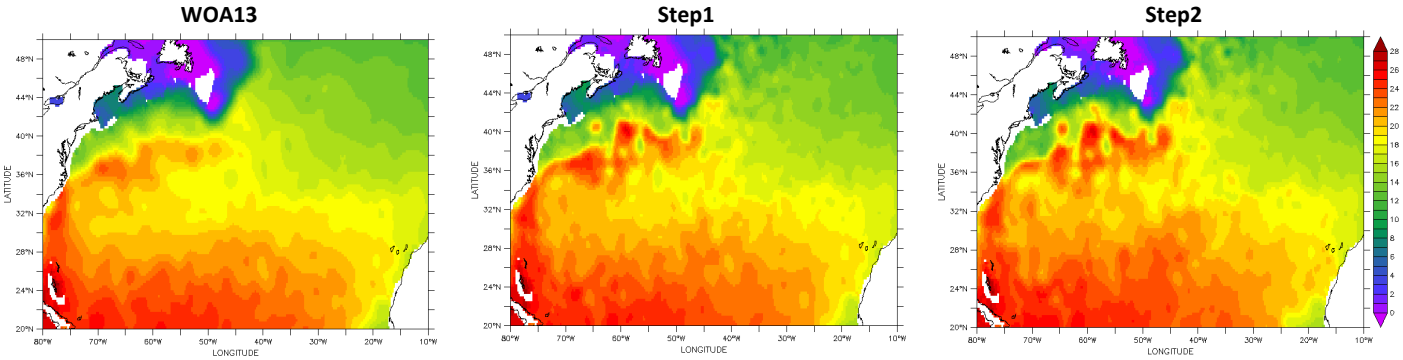

Figure 25: Temperature at 100 m from left to right: the first guess field (WOA13), the synthetic field (step1), the combined field (step2) for the 16th of August 2017 (in °C).

For the temperature field, the largest errors are found in the mixed layer depth (~0.35 °C). Then, the RMS differences decreases with depth. The bias is near zero and the residual error is about 5% of the signal variance whatever is the depth (Figure 26 left). For the salinity field, the largest errors are found from the surface down to the mixed layer depth (~0.045 psu). Then, as for the temperature field, RMS differences decreases with depth. The bias is also near zero and the residual error is also about 5% of the signal variance whatever is the depth (Figure 26 right).

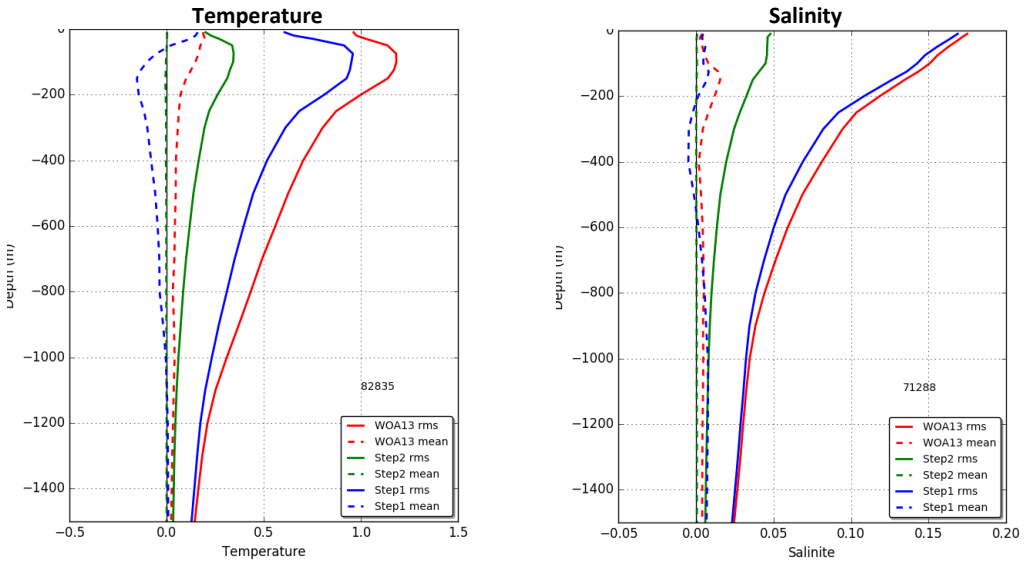

Figure 26: Global (solid line) Root Mean Square and (dashed line) Mean of the differences between the synthetic field (Step 1 - blue), the combined field (step 2 - green), the first guess WOA13 climatology (red) and in-situ T/S profiles for the August 2017 – July 2018 period. Temperature field (left) and salinity field (right).

4.3.2 DFS diagnostics

To assess the impact of the in-situ observations to map temperature and salinity fields together with the satellite observations and a first guess climatological field, Degree of Freedom of Signal (DFS) diagnostics are derived from ARMOR3D method. DFS diagnostics are influence matrix diagnostics and are directly available through the optimal interpolation method (Oke et al., 2015; Rémy et al., 2015). They provide a measure of the gain in information brought by the observations and they indicate furthermore if the analysis method considers having redundant information in a specific observing system.

DFS is calculated as the trace of the HK matrix, H being the observation operator and K the Kalman gain matrix. The optimal interpolation method used in the ARMOR3D system uses a Gauss-Markov estimator that provides a direct access to the HK matrix as it is explicitly computed along with the error covariance matrix or formal mapping error (Bretherton et al., 1976). DFS are computed on each HK matrix, meaning each grid point in case of a suboptimal optimal interpolation method. It is thus possible to use this metric to access the local mapping gain in information provided by each dataset (in-situ, synthetic…). Partial DFS are associated with a particular dataset and are computed from the partial trace of the HK matrix, taking only elements associated with the dataset to be analyzed. Partial DFS associated with the dataset i is written DFS(i). Two metrics have been particularly studied:

1- The fraction of the overall information coming from a given dataset (DFS(i)/ΣiDFS(i)),

2- The fraction of the information from the dataset exploited by the optimal interpolation method (i.e. the amount of information not lost to duplicate data and measurement error) (DFS(i)/N(i), N(i) being the actual number of observations from dataset i).

3 datasets have been considered in the analysis: the Argo observing system, the Other in-situ observations (including tropical moorings, XBT, CTD, etc) and the synthetic fields. Results show that most of the information comes from the Argo observing system, that the Other in-situ observations come second (where they are available) and that the synthetic fields fill the gap (Figure 27-left). This is fully consistent with the ingredients used in the optimal interpolation method since in addition to the conventional use of a measurement white noise applied to each of the observations, a spatially correlated error is additionally applied to the synthetic fields to take into account large-scale errors and bias introduced by the multiple linear regression method. Redundant information is found in the tropical oceans where the tropical moorings provide relatively high frequency observations compared to ARMOR3D weekly fields (Figure 27-right). Some regions like the Northern part of the Indian Ocean, the Japan Sea and the Eastern part of the tropical Pacific Ocean show also that there is some redundancy in the Argo observing system. This is linked to the way we use the in-situ observing system in the ARMOR3D method to correct the large-scale part of the synthetic fields.

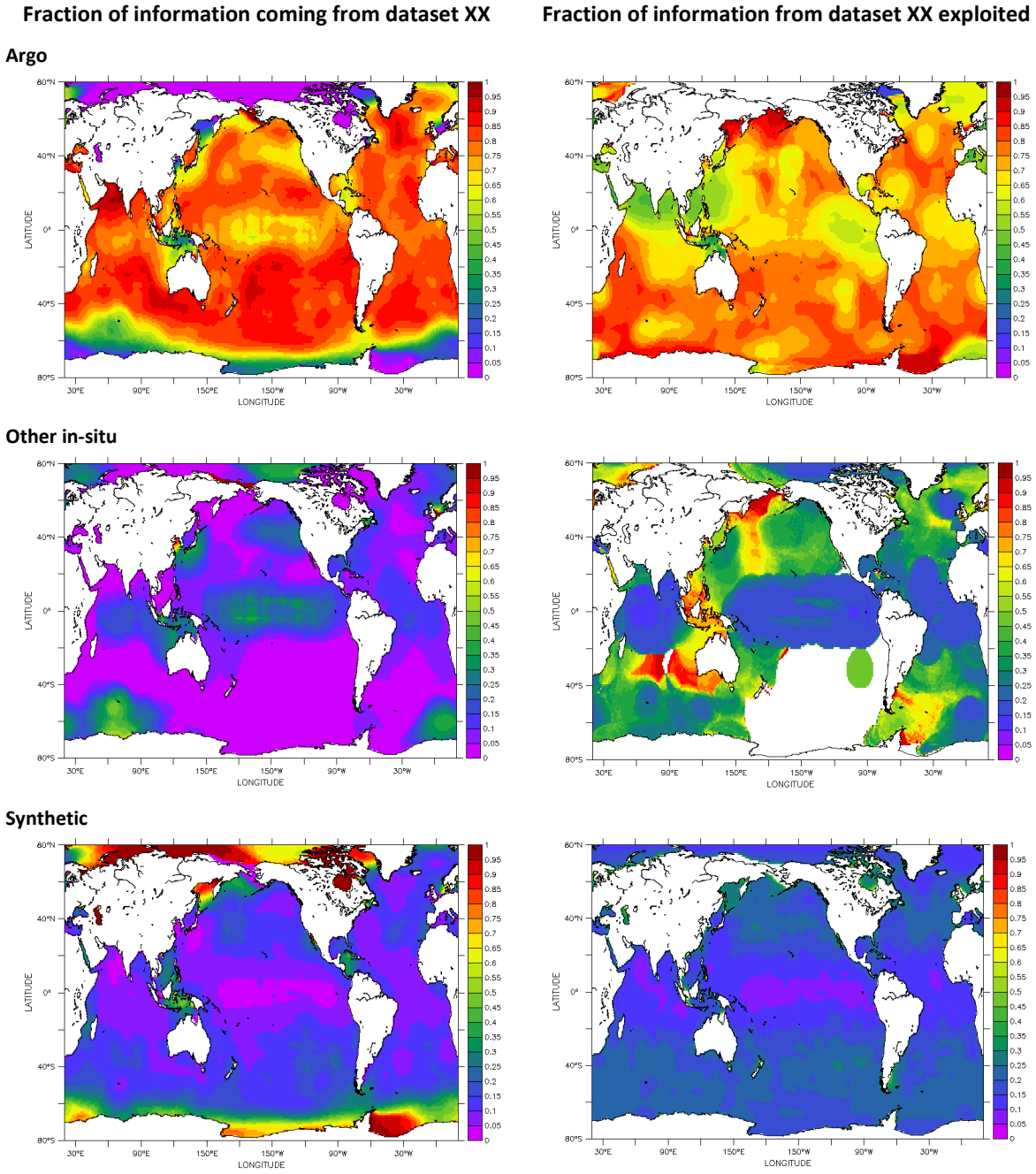

Figure 27: DFS metrics for the temperature field at 200m and the August 2017 – July 2018 period.

4.4 Impact of the Argo observing system

The impact of the Argo observing system is studied in the No Argo experiment. The No Argo experiment uses the same T&S in-situ profiles as the Reference experiment less the Argo floats (type PR_PF of product INSITU_GLO_NRT_OBSERVATIONS_013_030). This experiment although being very extreme allows quantifying the contribution of the Argo observations.

As for the Reference experiment, classical residual analysis with respect to T&S in-situ observations has been computed. Results (not shown) show very little differences between the synthetic (step1) and the combined (step2) fields. The contribution of the other in-situ observations, as global mean statistics, is very

small. Regional analysis shows however that their contribution is located where the other in-situ observations are situated (tropical moorings, along XBT/CTD lines, etc).
The contribution of the Argo observing system is further analysed by comparing the fields from the No Argo experiment with the fields obtained from the Reference experiment. The Argo observations allow correcting the bias that exists in the first guess field (WOA13). The amplitude of the bias and its geographical distribution vary between the temperature and the salinity fields and as a function of depth (Figure 28, Figure 29). A fresh bias is clearly visible at almost all depths with a global mean value of 0.008 psu and with values up to 0.1 psu in the North Atlantic Ocean at 1000m depth. The temperature bias is mostly negative at the surface and then becomes mostly positive bellow 100m depth with values up to 1°C in the Tropical Atlantic and Pacific Oceans.

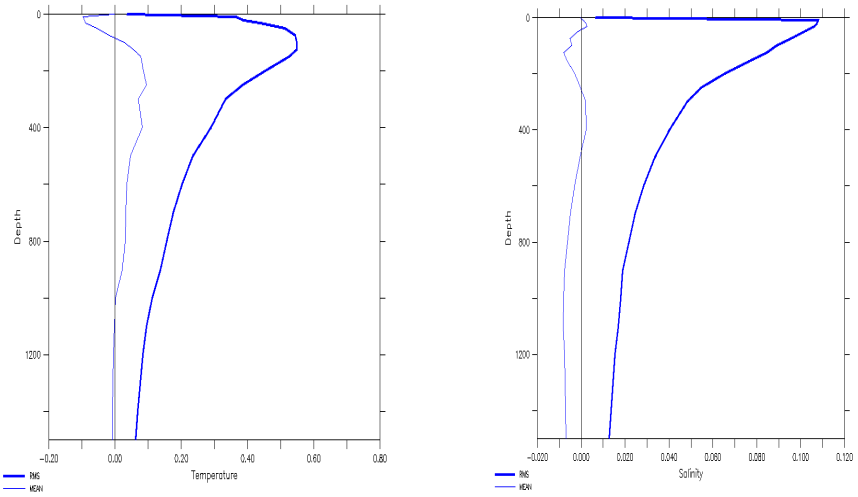

Figure 28: Global (bold line) Root Mean Square and (thin line) Mean of the differences between the No Argo experiment and the Reference experiment for the August 2017 – July 2018 period. Temperature field (left) and salinity field (right).

In term of RMS difference with the Reference experiment (Figure 28), the largest improvements are found in the mixed layer for the temperature with a global mean value of 0.5°C and just below the surface for the salinity with a global mean value of 0.105 psu. The RMS difference with the Reference experiment decreases then progressively as the depths increase to value around 0.18°C for the temperature field and 0.012psu for salinity. This is very consistent with what has been described from Figure 26.

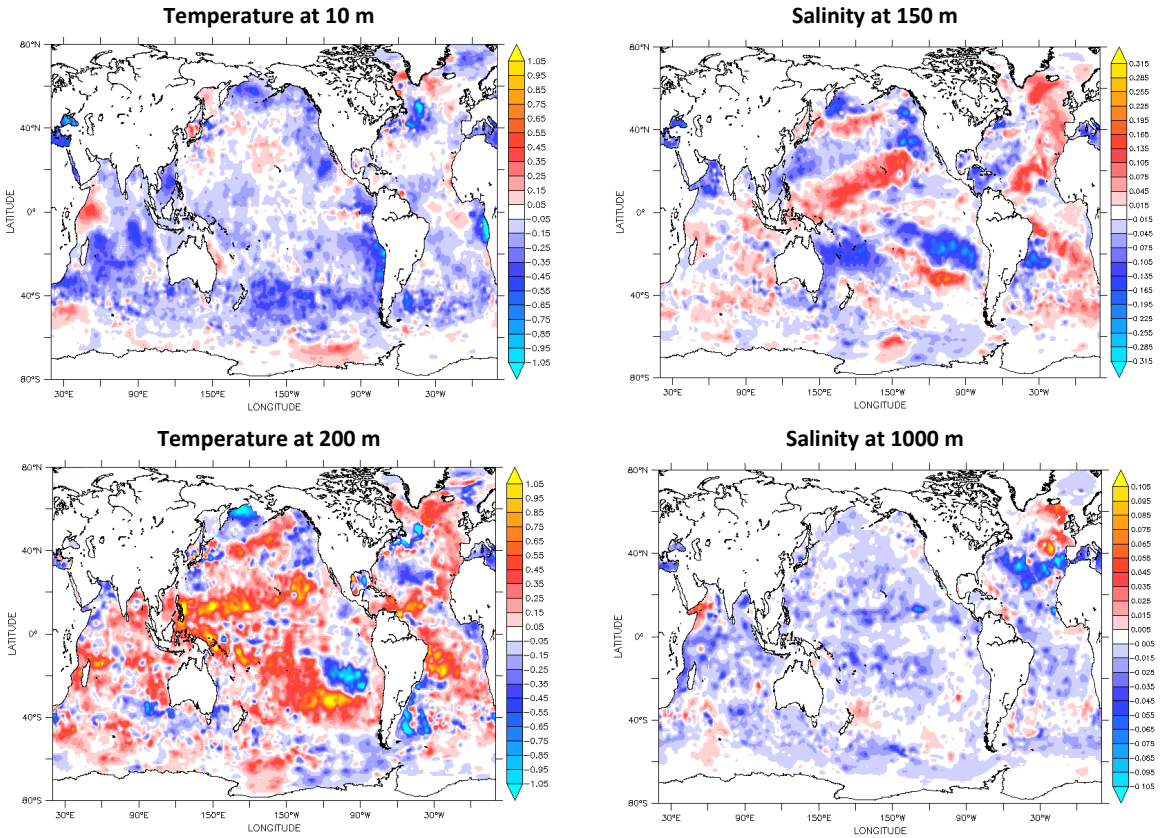

Figure 29: Mean difference between the No Argo experiment and the Reference experiment for the Temperature (left) and Salinity (right) fields at different depths. Statistics are calculated for the August 2017 – July 2018 period.

4.5 Impact of deep Argo observing system

The impact of the Deep Argo observing system is studied in the Deep Argo experiment. The Deep Argo experiment uses the same T&S in-situ profiles as the Reference experiment plus the Deep Argo floats. 1800 Deep Argo T/S profiles are available between July 2017 and August 2018 (QC='3' are kept, QC='4' are rejected) (Figure 24).

The contribution of the Deep Argo observing system is analysed by comparing the fields from the Deep Argo experiment with the fields obtained from the Reference experiment. As for recent OSSEs experiments conducted also in the frame of the AtlantOS project to study enhancement of the Argo Observing System to full depth sampling (Guinehut, 2018), results show that the Deep Argo observations allow first to correct the bias that exists at depth in the first guess fields (WOA13 climatology) (Figure 30, Figure 31). The bias is mostly positive for the temperature field and of the order of 0.05°C in most areas. The bias is fresh for the salinity and of the order of 0.005 psu in most areas with also positive values of the same amplitude in the South Indian and Pacific Oceans. In term of RMS difference with the Reference experiment, global mean values are between 0.002°C and 0.003°C for the temperature field and between 0.0004psu and 0.0006psu for salinity (Figure 30).

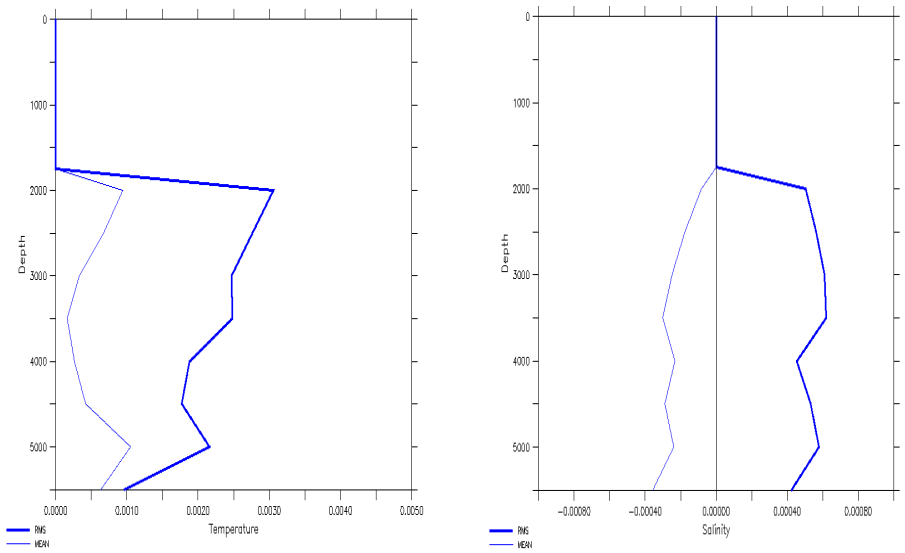

Figure 30: Global (bold line) Root Mean Square and (thin line) Mean of the differences between the Deep Argo experiment and the Reference experiment for the August 2017 – July 2018 period. Temperature field (left) and salinity field (right).

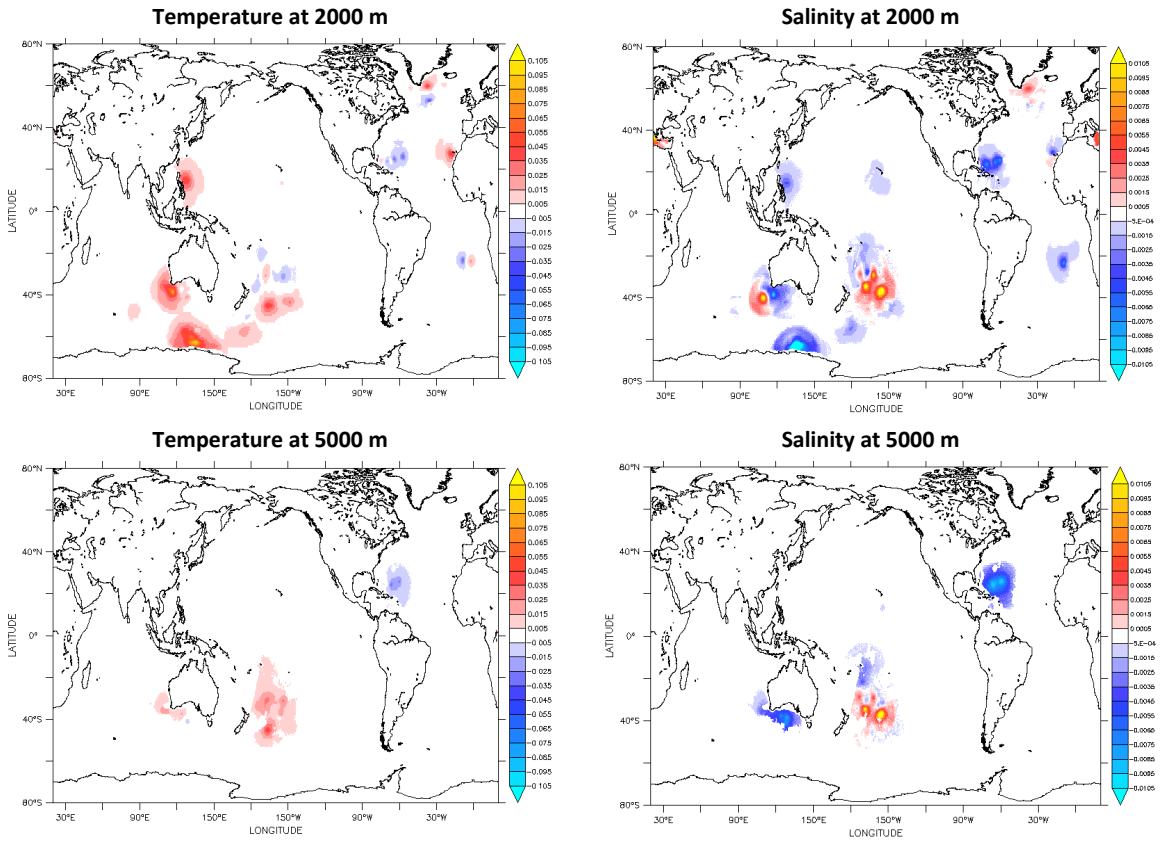

Figure 31: Mean difference between the Deep Argo experiment and the Reference experiment for the Temperature (left) and Salinity (right) fields at 2000m and 5000m. Statistics are calculated for the August 2017 – July 2018 period.

4.6 Synthesis and perspectives

The impact of the different observing system (satellite versus in-situ) and more specifically of the Argo and Deep Argo observing systems on ocean state estimate has been studied using the ARMOR3D multivariate analysis system. The studies have been performed over a 1-year period between August 2017 and July 2018.

Results show that the in-situ observations, and specifically the Argo observing system which provides regular and global sampling of the ocean, allow first to correct the bias that exist in the a priori knowledge of the ocean state (i.e. the first guess fields based on a climatology in our case). The amplitude of this bias and its geographical distribution vary between the temperature and the salinity fields and as a function of depth. The Argo observations allow of course also a better restitution of the variability of the fields together with space borne observations. These results confirm the invaluable value of the Argo observing system.

Perspectives include longer time scales (e.g. 2 to 3 years) analysis as well as the refinement of the ingredients of the method (i.e. error covariance matrix applied to the different observations, spatial and temporal correlation scales) which have not been modified compared to the operational ARMOR3D chain, to make best use of the new/sparse Deep Argo observations.

5 Impact of AtlantOS in-situ observations on seasonal prediction

5.1 Description of work and setup

ECMWF carried out a number of seasonal forecasting experiments to assess the impact of ocean in-situ observations on the forecast quality. Forecast quality has been assessed with standard metrics such as RMSE and Canonical Correlation Analysis (CCA; see e.g. Wilks 2011). CCA can be used to detect regions that are sensitive to uncertainties or differences in the initial conditions.
The seasonal forecast experiments described here used ECMWF's current seasonal prediction system SEAS5 (Stockdale et al. 2018) ran at the operational resolution TCO319 (~32km) in the atmosphere and at a lower-than-operational 1 degree horizontal with 42 vertical levels in the ocean. Ocean initial conditions were taken from five Observing System Experiments (OSE), in which ocean reanalyses were performed with different in-situ observation types removed globally (Zuo et al., 2019). The OSEs were based on a low-resolution version (1 degree horizontal with 42 vertical levels) of ECMWF's new ocean reanalysis ORAS5 (Zuo et al. 2018; see also report D1.5 for details and results).

Based on these five OSEs, five re-forecast experiments have been conducted: REF (all in-situ data retained), NoArgo (no Argo float observations), NoMoorings (no moored buoys data including Tropical Mooring arrays), NoXBT (no XBT/MBT and CTD observations), NoInsitu (no in-situ observations, i.e. no Argo, moored buoys, XBT/MBT, CTD data). Each re-forecast experiment covers the period 1993-2015 with two start dates every year (May and November), with each forecast covering 7 months and comprising 15 ensemble members.
To statistically derive spatial maps of sensitivities of the seasonal forecast experiments to changes in ocean initial conditions, CCA has been implemented as a diagnostic tool. CCA aims to seek temporally coherent (so-called canonical) patterns of variability in predictor and predictand fields, yielding also time series of the temporal evolution of these patterns. As described in D1.5, this technique is most powerful when applied to differences between systems, since in this way the focus is on the impact of the specific differences between two experiments, and skill variations that are common to both systems are eliminated by construction.

5.2 Changes in sea surface temperature in re-forecast experiments

Figure 32 shows changes in RMSE of sea surface temperature (SST) forecasts for DJF (initialized in November) in the different re-forecast experiments. Positive (Negative) values mean degradation (improvement) of the forecasts with respect to REF. Overall, removal of in-situ observing systems from the ocean initial conditions degrades the SST forecasts in (in order of increasing impact) NoXBT, NoArgo, and NoInsitu, with maximum values in the Gulf Stream and Kuroshio regions, but changes are also present in the equatorial oceans. The RMSE changes in NoMoorings are comparatively small. The RMSE values shown in Figure 32 are not calibrated (i.e. the bias is not removed before computation). Hence, they include effects from changes in both mean (bias) and standard deviation of forecast errors.

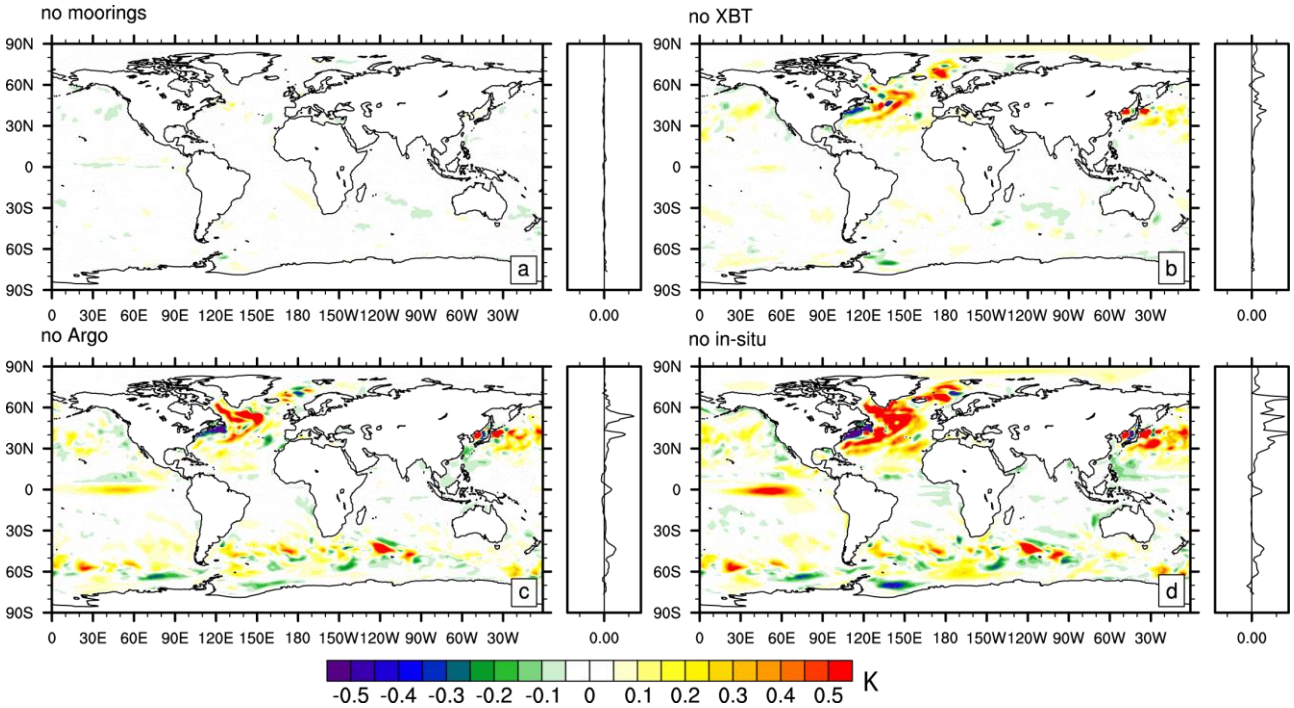

Figure 32: Change in ensemble mean RMSE of DJF seasonal forecast SST in a) NoMooring, b) NoXBT, c) NoArgo, and d) NoInsitu with respect to REF for 1993-2015. The zonal average plots range from -0.15K to 0.15K. The reference reanalysis REF was used as verifying data set.

Changes in bias-corrected RMSE (BCRMSE) of DJF SST forecasts are shown in Figure 33. Here it is clearer where forecast skill is degraded when in-situ systems are removed. Main areas of degradation are the North Atlantic Gulf Stream region and the eastern equatorial Pacific SST, the latter indicating degraded forecasts of El Nino-Southern Oscillation (ENSO) when Argo or all in-situ systems are removed. Changes in the tropical Atlantic and Indian Oceans are more neutral, indicating that the negative values seen for RMSE changes in these regions (Figure 32) are due to a bias reduction. One possibility is that the mean ocean states of these regions in reanalyses are well constrained by sea surface observations (SST and sea-level) even without in-situ observations. Further investigation is needed though. Another surprising effect is the slightly improved BCRMSE in the Southern Ocean in NoArgo and NoInsitu, indicating that the information from Argo is possibly not optimally used in the system, at least not in the low-resolution setup used here.

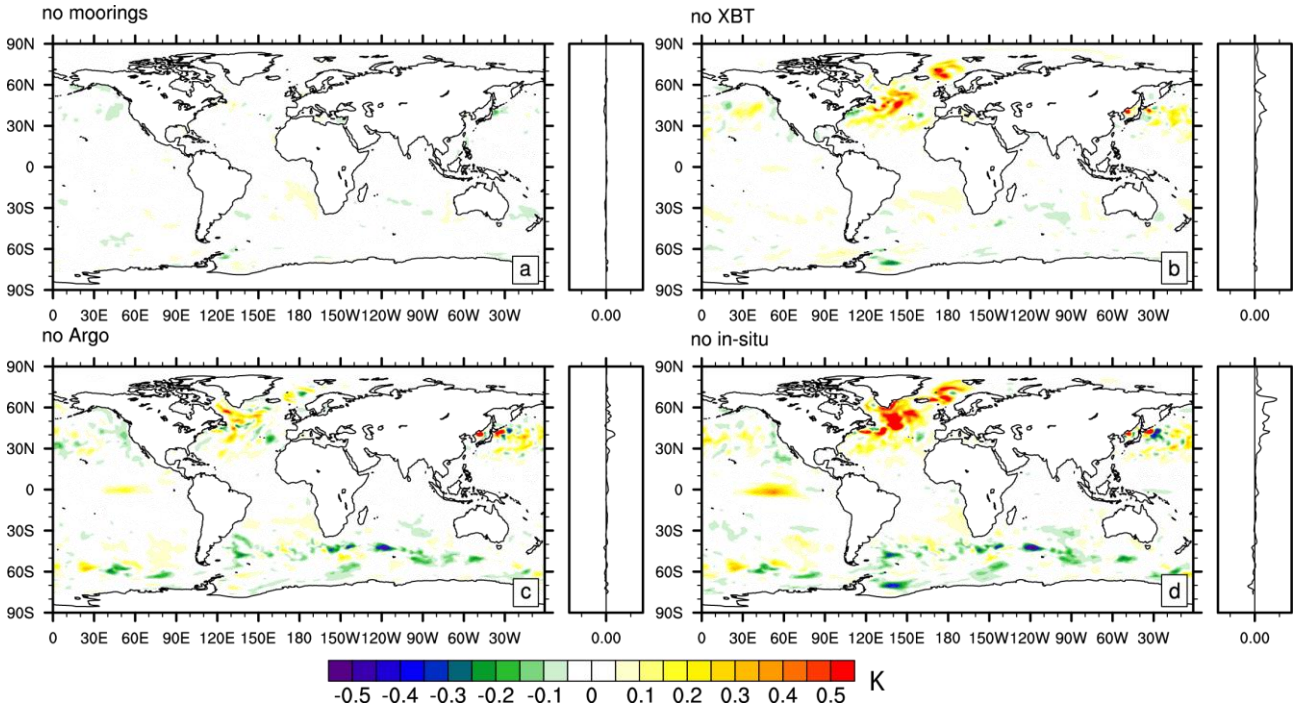

Figure 33: As in Figure 31 but with the mean forecast bias removed from every seasonal forecast experiment: change in ensemble mean bias-corrected RMSE of forecast DJF SST in a) NoMooring, b) NoXBT, c) NoArgo, and d) NoInsitu with respect to REF for 1993-2015. The zonal average plots range from -0.15K to 0.15K. The reference reanalysis REF was used as verifying data set.

Results for re-forecasts initialized in May (not shown) indicate SST forecast degradation of generally similar magnitude, but the changes are larger (smaller) in the Southern (Northern) Hemisphere extratopics compared to the November starts shown in Figure 32 and Figure 33. This indicates that forecasts in the respective winter hemisphere are more sensitive to removal of ocean observing systems.

We also note that calibration of forecasts has proven problematic for the present experiments because of the non-stationarity of the biases due to temporal changes in the different observing system. The a-posteriori bias correction works better for systems with a stationary bias such as our experiment without any in-situ observations, since it is not affected by discontinuities in the observing system. As a consequence, the BCRMSE in systems with a changing observing system (most notably Argo) and associated changes in biases may be overestimated. Thus, bias-corrected RMSE in systems with different bias evolution should be compared only with caution.

5.3 Atmospheric impacts

In this section we explore the atmospheric impact of the changes in SST predictions that we discussed in the previous section. Changes in BCRMSE of DJF forecasts of relevant atmospheric quantities in the NoInsitu experiment are presented in Figure 34.

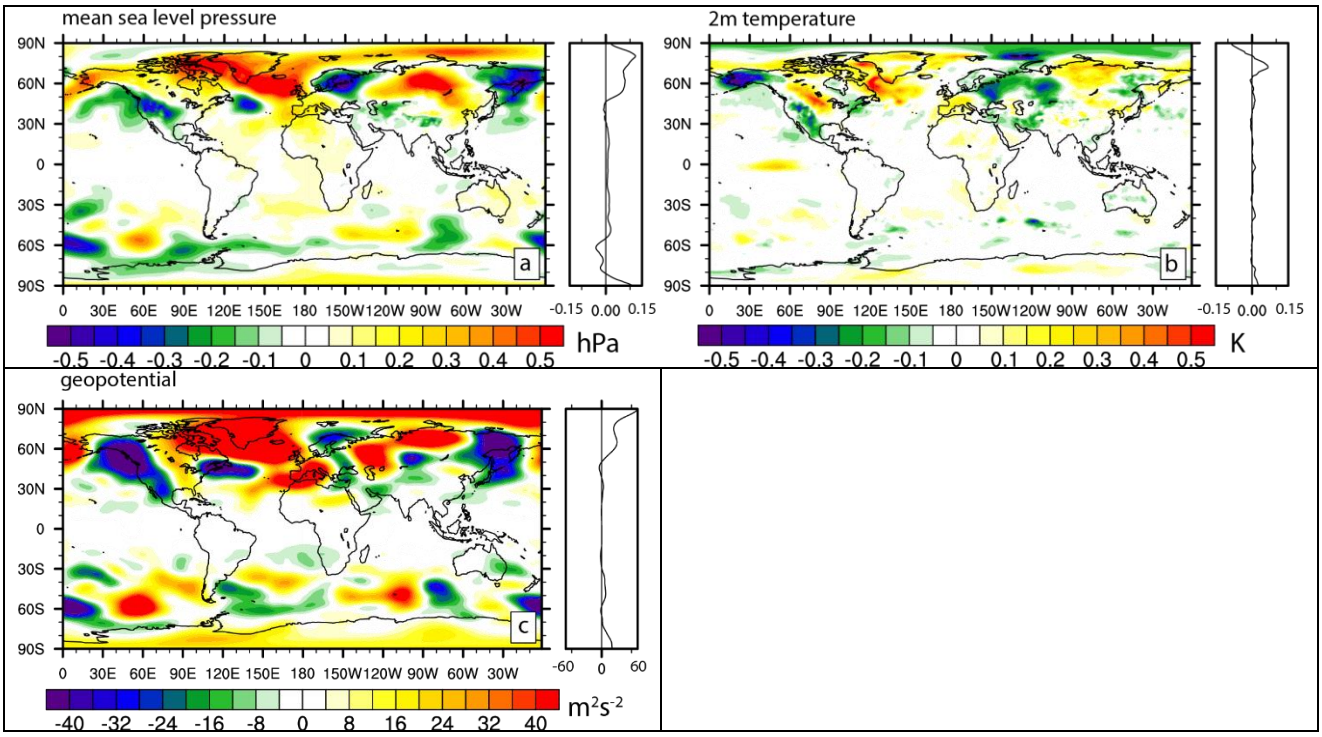

Figure 34: ***Changes in ensemble mean BCRMSE for DJF forecasts of atmospheric fields in NoInsitu relative to REF: a) mean sea level pressure, b) two-metre temperature, c) 500hPa geopotential. ERA-Interim was used as verifying data set.***

Two-metre temperature skill reduction (Figure 34 b) is co-located with skill reduction in SST (Figure 32 d), but there are also downstream effects, especially in the Northern Hemisphere. They are represented by a wavenumber 2 pattern in skill changes in two-metre temperature, with a positive (i.e. degraded) zonal average. This wave-like pattern in skill changes is also present in mean sea level pressure (Figure 34) and 500hPa geopotential (Figure 34 c). The Northern Hemisphere zonal average BCRMSE changes are positive for the latter quantities, indicating a degradation of the position of the planetary waves in NoInsitu. Whether these changes are driven remotely from the tropical Pacific via ENSO teleconnections or the North Atlantic is under investigation with regionalized OSEs and associated re-forecast experiments.

As for the SSTs, atmospheric impacts in JJA re-forecasts (May start dates; not shown) are stronger in the Southern Hemisphere extratropics, where the NoInsitu experiment exhibits similar skill degradation as found for the Northern Hemisphere in DJF (as shown in Figure 34).

We now turn to results from the CCA diagnostics. As explained in the section about SST changes, we use differences in ocean initial conditions (i.e. differences between the different OSEs used for initializing the forecast experiments) as a predictor for differences in the forecasts of various atmospheric fields in the following season (lead month 2-4). The latter can be interpreted as patterns of forecast sensitivity to difference patterns in the ocean initial conditions.

Figure 35 a shows CCA results using differences in SST initial conditions between NoArgo and REF (=ΔSST) in May as predictor and differences in JJA forecasts of two-metre temperature (=ΔT2m) as predictand. In practice, the ΔSST and ΔT2m fields have first been decomposed into their first 10 EOFs, retaining 90% and 87% of variance of the input fields, respectively. The CCA has then been applied to the 2x10 Principal Components (PC) that resulted from the EOF analysis. The first canonical predictand field of ΔSST (**g1** in Figure 35 a) retains 31% of the total variance explained by the first 10 EOFs and exhibits generally positive values which are largest south of the equator. The RMS value of the ΔSST field reconstructed only from this first canonical pattern is sqrt(0.31*0.06^2)~0.03K. The associated time series **u1** (see bottom panel in Figure 35 a) is almost constant during the first years and then starts to decline and to eventually change sign from ~2003 onward. This indicates that, with the advent of Argo, initial conditions in NoArgo became gradually cooler compared to REF. Thus, Argo observations acted to increase SSTs in REF in this region. The first canonical predictand pattern of ΔT2m (**h1** in Figure 35 a) exhibits spatial patterns and a temporal evolution

(**v1,** see bottom panel in Figure 35 a) that are very similar to ΔSST showing the strong coupling of T2m with underlying SSTs. There is also some indication that positive ΔSST values are propagated to ΔT2m over the adjacent continents. The magnitude of ΔT2m is larger than that of ΔSST [RMS value of field reconstructed from **h1** is sqrt(0.29*0.18^2)~0.1K], which is mainly related to the amplification of ΔSST during the forecast.

Performing a CCA for 850hPa temperature instead of T2m yields qualitatively similar results, but with lower magnitude (not shown).

Figure 35 b shows CCA results using also ΔSST in May as predictor but the difference in precipitation (Δprecip) in JJA as predictand. The resulting canonical predictor pattern of ΔSST (**g1** in Figure 35 b) is indistinguishable from that in Figure 35 a, and also the represented variance is very similar. However, the corresponding predictand pattern of Δprecip (**h1** in Figure 35 b) nicely shows how the position of the Intertropical Convergence Zone (ITCZ) reacts to the changed cross-equatorial SST gradient. It shows a band of negative values north of the equator and positive values along the equator, indicating that the ITCZ moves southward, towards the warmer SSTs. Specifically, SSTs in NoArgo become gradually cooler compared to REF (time series **u1** in Figure 35 b turns negative), leading to a more northerly position of the ITCZ compared to REF (compare **v1** in Figure 35 b). Conversely speaking, Argo observation tend to warm SSTs in the southern tropical Atlantic and lead to a more southerly position of the ITCZ. Signals over the African continent indicate that these results also have implications for forecasts of the African monsoon.

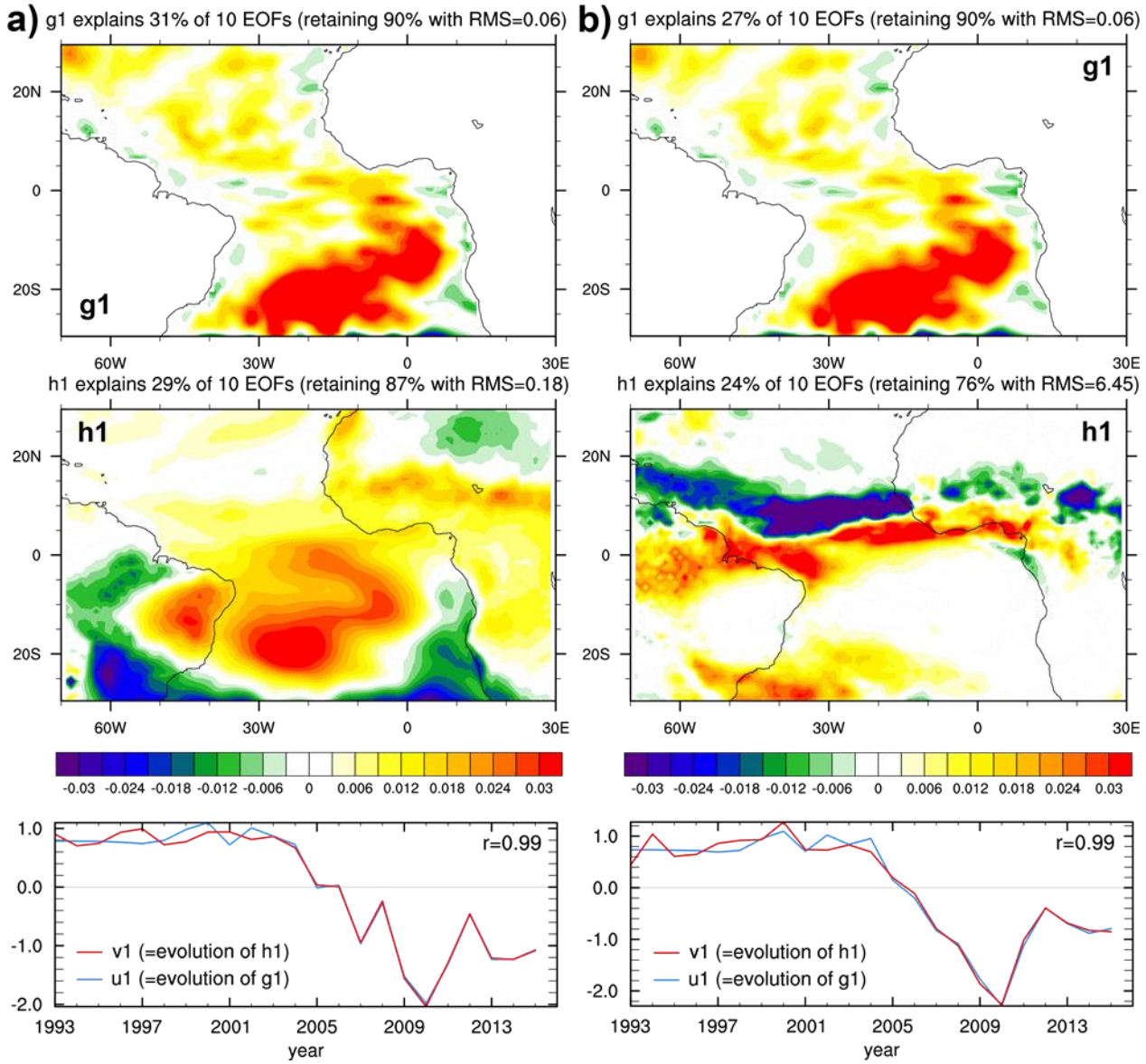

Figure 35: ***CCA applied to differences between NoArgo and REF using SST differences in May as predictor and (a) (left column) two-metre temperature and (b) (right column) precipitation as predictand. First canonical predictor (predictand) patterns are represented by g1 (h1). Time evolution of g1 (h1) is represented by the curves u1 (v1). Fields and time series are normalized. Values in brackets denote the fraction of variance retained by the 10 EOFs underlying the CCA analysis and, as an indication of magnitude, the RMS value of the field reconstructed from these 10 EOFs. Units of underlying precipitation fields are mm/month.***

CCA diagnostics yielded qualitatively similar results for other experiments and seasons, although the spatial patterns and temporal evolution are naturally different for each observing system (not shown). Specifically, we found a strong sensitivity of the ITCZ position to the cross-equatorial SST gradient for all experiments, which demonstrates the remote effect of reduced observational coverage.

6 Conclusion

This report focuses on the impact of AtlantOS *in situ* observations on near real time ocean analysis and seasonal forecast delivered respectively by the Copernicus Marine Service and ECMWF.

Several impact assessment methods have been deployed by the different partners:

- Observing System Experiments (OSE): ocean analysis with and without part of the in situ network observations have been removed are compared,
- Degree of Freedom of the System (DFS) which gives an indication of the observation information used by the analysis,
- Canonical-correlation analysis (CCA) allowing to statistically derive spatial maps of sensitivities of the seasonal forecast experiments to changes in ocean initial conditions.

The spread of CMEMS Global Reanalysis Ensemble Project (GREP) based on four reanalysis is used to quantitatively and regionally characterize temperature and salinity uncertainties in the analysis.

For some in situ observing network, impact analysis was carried out with several CMEMS systems, allowing intercomparison of their impact. This was the case for the deep Argo profilers and surface drifters.

The deep Argo pilot array is still at an early stage of deployment and only few profilers are already deployed. Their assimilation is still promising with positive impact in the different ocean analysis systems. It has been recognized by the oceanography community that more intensive sampling in the deep ocean is needed, and this is illustrated by the spread of the GREP reanalyses to represent the time-mean and the variability. The deep Argo temperature and salinity observation assimilation reduces the model minus observations difference by more than 50% at the point location, in both MetOffice and Mercator Ocean ocean analysis. This is in agreement with results of the AtlantOS Task 1.3, which demonstrate that the implementation of global deep Argo array composed of 1300 floats would provide a significant constrain to the deep ocean (Gasparin et al., 2019). Due to the very sparse coverage of the present deep Argo array, the influence of their deep observations is local (ARMOR3D, MetOffice and Mercator Ocean analysis). With an improved regular and global coverage, we can expect a significant forecast error reduction below 2000 m depth in both temperature and salinity from the Argo deep fleet.

The surface drifter network is composed of around 1500 instruments that provide in near real time surface ocean temperature at an hourly frequency, at global scale. It has been shown with the MetOffice system that removing half of all drifters causes an increase in the upper ocean temperature RMSE by >20% across a large fraction of the global ocean, focussed on the mid latitudes where there are a significant number of existing drifters. In the Mercator Ocean system, the comparison to mooring time series shows a slight benefit to the system, even if the model minus drifter SST is significantly reduced with their assimilation.
Those impact experiment with the drifters highlight the difficulty to validate the change seen in the analysis by their assimilation as the satellite SST product, assimilated or used for validation, could have been debaised with the drifter SST. The in situ data are often too sparse to obtain robust regional statistic over a short period.

The impact of ocean in situ network assimilation on seasonal forecast was assessed by using different initial ocean conditions that have seen only part of the in situ network. It was shown that the removal of in-situ observing systems from the ocean initial conditions degrades the SST forecasts with maximum values in the Northern Atlantic and Kuroshio regions, but changes are also present in the equatorial oceans, mostly in the Pacific.

A canonical analysis was conducted to assess the impact of changes in the ocean in situ network on the atmosphere. This analysis highlights a strong sensitivity of the Intertropical Convergence Zone (ITCZ) position to the cross-equatorial SST gradient for all experiments, which demonstrates the remote effect of reduced observational coverage.

The AtlantOS project gave us a good vision of the full value chain from the individual observing networks to the data integrators and the Copernicus Ocean monitoring and seasonal coupled ocean/atmosphere forecasting systems.
Within the WP7, we had the opportunity to interact together and reinforce the links between the observing networks, the data integrators and the operational systems but also within the operational systems themselves. The need and benefit of such interactions and integrated view is now better recognized.
This will continue beyond the end of the AtlantOS project in different context (CMEMS, EuroSea, Ocean Predict, TPOS2020, Argo, PIRATA…)

The analysis of the data assimilation experiments done to assess the observation impact revealed some room for improvements. The use of multiple systems helped to better interpret the results. Further developments within the operational systems have already been done and others will be conducted to improve the benefit of individual observing networks with more specific treatments for each of them. Some of those developments will undergo under CMEMS or H2020 projects such as EuroSea. They aim at coordinating activities on a better use of present observations in operational systems and refinement of network extension requirements.
For seasonal forecasts, the impact of using different ocean initial conditions assimilating different sets of ocean observations was assessed. The results were sometimes mitigated. Further analysis of the different experiments is ongoing to better understand those results. This should greatly benefit to the next S2S systems with a better comprehension on how the ocean initial conditions “influence” the seasonal coupled forecast.

There was also a strong communication effort in and outside AtlantOS that will continue at international level on observation impact studies. This aims at promoting those activities and enhances the cooperation between the observing systems and the operational systems to better integrate the in situ observations.

References

Amante, C., Eakins, B.W., 2009. ETOPO1 1 arc-minute Global Relief Model: Procedures, Data Sources and Analysis. US Department of Commerce, National Oceanic and Atmospheric Administration, National Environmental Satellite, Data, and Information Service, National Geophysical Data Center, Marine Geology and Geophysics Division Colorado.

Becker, J.J., Sandwell, D.T., Smith, W.H.F., Braud, J., Binder, B., Depner, J., Fabre, D., Factor, J., Ingalls, S., Kim, S.H., 2009. Global bathymetry and elevation data at 30 arc seconds resolution: SRTM30_plus. Mar. Geod. 32, 355–371.

Brasseur, P., Verron, J., 2006. The SEEK filter method for data assimilation in oceanography: a synthesis. Ocean Dyn. 56, 650–661.

Bretherton, F. P., R. E. Davis and C. B. Fandry, A technique for objective analysis and design of oceanographic experiments applied to MODE-73, 1976 / *Deep-Sea Res*., 23, 559-582.

Desbruyères, D.G., Purkey, S.G., McDonagh, E.L., Johnson, G.C., King, B.A., 2016. Deep and abyssal ocean warming from 35 years of repeat hydrography. Geophys. Res. Lett. 43.

Gasparin F., S. Guinehut C., Mao, I. Mirouze, E. Remy, R. King, M. Hamon, R. Reid., A. Storto, P.Y. Le Traon, M. Martin and S. Masina (2018). Requirements for an integrated in situ Atlantic Ocean Observing System from coordinated Observing System Simulation Experiments, Frontiers in Marine Sciences, In Review

Gasparin F., Hamon, M., Remy, E., and P.Y. Le Traon (2019). Towards robust estimations of the deep ocean variability with deep Argo. J. Climate, to be submitted.

Good, S.A., Martin, M.J., Rayner, N.A., 2013. EN4: quality controlled ocean temperature and salinity profiles and monthly objective analyses with uncertainty estimates. J. Geophys. Res. Oceans 118, 6704–6716.

Guinehut S., A.-L. Dhomps, G. Larnicol and P.-Y. Le Traon, 2012: High resolution 3D temperature and salinity fields derived from in situ and satellite observations. Ocean Sci., 8, 845-857, doi:10.5194/os-8-845-2012.

Guinehut S., 2018: OSSE results using the multivariate ARMOR3D data analysis system, Appendix C to report D1.5 of the European H2020 AtlantOS project (N° 633211).

Kouketsu, S., Kawano, T., Masuda, S., Sugiura, N., Sasaki, Y., Toyoda, T., Igarashi, H., Kawai, Y., Katsumata, K., Uchida, H., 2011. Deep ocean heat content changes estimated from observation and reanalysis product and their influence on sea level change. J. Geophys. Res. Oceans 116.

Lellouche, J.M., Le Galloudec, O., Drévillon, M., Régnier, C., Greiner, E., Garric, G., Ferry, N., Desportes, C., Testut, C.E., Bricaud, C., 2013. Evaluation of global monitoring and forecasting systems at Mercator Océan. Ocean Sci. 9, 57.

Lellouche, J.M., Greiner, E., Le Galloudec, O., Garric, G., Regnier, C., Drevillon, M., Benkiran, M., Testut, C.E., Bourdalle-Badie, R., Gasparin, F., Hernandez, O., Levier, B., Drillet, Y., Remy, E., Le Traon, P.Y., 2018. Recent updates on the Copernicus Marine Service global ocean monitoring and forecasting real-time 1/12 high resolution system. Ocean Sci. Discuss. 2018, 1–70. http://dx.doi.org/10.5194/os- 2018-15.

Locarnini, R. A., A. V. Mishonov, J. I. Antonov, T. P. Boyer, H. E. Garcia, O. K. Baranova, M. M. Zweng, C. R. Paver, J. R. Reagan, D. R. Johnson, M. Hamilton, and D. Seidov, 2013. World Ocean Atlas 2013, Volume 1: Temperature. S. Levitus, Ed., A. Mishonov Technical Ed.; NOAA Atlas NESDIS 73, 40 pp.

Lumpkin, R., Özgökmen, T., and Centurioni, L. (2017). Advances in the applications of surface drifters. *Ann. Rev. Mar. Sci.* 9, 59–81. doi: 10.1146/annurev-marine-010816-060641

Madec, G., the NEMO team, 2008. Nemo ocean engine: note du pole de modélisation. In: Tech. Rep. Institut Pierre-Simon Laplace (IPSL), France, pp. 1288–1619 No 27 ISSN No.

Oke P. R., G. Larnicol, Y. Fujii; G. C. Smith, D. J. Lea, S. Guinehut, E. Remy, M. A. Balmaseda, T. Rykova, D. Surcel-Colan, M. J. Martin, A. A. Sellar, S. Mulet and V Turpin, 2015: Assessing the impact of observations on ocean forecasts and reanalysis: Part 1, Global studies. Journal of Operational Oceanography, 8:sup1, s49-s62, doi: 10.1080/1755876X.2015.1022067.

Purkey, S.G., Johnson, G.C., 2010. Warming of Global Abyssal and Deep Southern Ocean Waters between the 1990s and 2000s: Contributions to Global Heat and Sea Level Rise Budgets*. Journal of Climate 23, 6336–6351.

Rémy E., V. Turpin and S. Guinehut, 2015: Global ocean analysis and forecasting: OSE/OSSEs results and recommendations. Report D3.313 of the European FP7 E-AIMS project (N° 284391).

Rio, M.H., Mulet, S., Picot, N., 2014. Beyond GOCE for the ocean circulation estimate: synergetic use of altimetry, gravimetry, and in situ data provides new insight into geostrophic and Ekman currents. Geophys. Res. Lett. 41, 8918–8925.

Stockdale, T., and Coauthors, 2018: SEAS5 and the future evolution of the long-range forecast system. ECMWF Tech Memo, 835.

Turpin V., Remy E., Le Traon Pierre-Yves, 2016: How essential are Argo observations to constrain a global ocean data assimilation system? Ocean Science, 12(1), 257-274. https://doi.org/10.5194/os-12-257-2016.

Wilks, D. S., 2011: Statistical methods in the atmospheric sciences. Academic press,.

Zuo, H., M. A. Balmaseda, K. Mogensen, and S. Tietsche, 2018: OCEAN5: the ECMWF Ocean Reanalysis System and its Real-Time analysis component. ECMWF Tech Memo, 823.

Zuo, H., Balmaseda, M.A, Tietsche, S., Mogensen, K., Mayer, M., deRosnay, P. 2019: The ECMWF operational ensemble reanalysis-analysis system for ocean and sea-ice: a description of the system and assessment. Ocean Science, in preparation.

Zweng, M.M, J.R. Reagan, J.I. Antonov, R.A. Locarnini, A.V. Mishonov, T.P. Boyer, H.E. Garcia, O.K. Baranova, D.R. Johnson, D.Seidov, M.M. Biddle, 2013. World Ocean Atlas 2013, Volume 2: Salinity. S. Levitus, Ed., A. Mishonov Technical Ed.; NOAA Atlas NESDIS 74, 39 pp.